

## ABSTRACT

Title of Document:                    BIOCHEMICAL CHARACTERIZATIONS  
  OF EXTRACELLULAR VESICLES SHED  
  BY VEGETATIVE AND SPORULATING  
  *BACILLUS SUBTILIS*

**Yeji Kim, Master of Science, 2015**

Directed By:                            Professor Catherine Fenselau,  
  Department of Chemistry and Biochemistry

Sporulation of *Bacilli* is a developmental process that provides long-term viability in unfavorable environments. Recently, biogenesis of extracellular vesicles (EVs) from *Bacilli* has also been reported to participate in various physiological and pathogenic phenomena. In this study, EVs were isolated from vegetative and sporulating *Bacillus subtilis* cells and characterized using mass spectrometry (MS)-based proteomics, microscopy, and fluorescence spectrophotometry. The microscopic approach demonstrated that both vegetative and sporulating cells produce EVs. In the proteomic analysis, 156 proteins were identified with statistical significance in EVs

collected at the vegetative phase and 185 proteins in EVs shed during sporulation. The two EV cargos showed qualitatively and quantitatively different proteome patterns. Sporulation-associated proteins had greater abundances in EVs at the sporulation stage. Additionally, a fusion-like event of EVs with *B. subtilis* cells was observed by a fluorescence de-quenching assay. Based on these observations, *B. subtilis* EVs are proposed to support intercellular communication and sporulation.

BIOCHEMICAL CHARACTERIZATIONS OF EXTRACELLULAR VESICLES  
SHED BY VEGETATIVE AND SPORULATING *BACILLUS SUBTILIS*

By

Yeji Kim

Thesis submitted to the Faculty of the Graduate School of the  
University of Maryland, College Park, in partial fulfillment  
of the requirements for the degree of  
Master of Science  
2015

Advisory Committee:  
Professor Catherine Fenselau, Chair  
Professor Jason Kahn  
Professor Shuwei Li

© Copyright by

Yeji Kim

2015

## Acknowledgements

It is my great pleasure to acknowledge invaluable help from all the people because of whom I could complete the work presented in this thesis. First and foremost, I wish to thank my advisor, Prof. Catherine Fenselau, for her continuing guidance, support, inspiration and many more. She introduced me to the infinite pleasure of scientific research. Her uncountable advices and constructive criticisms have always encouraged me to make progress in my research work. In addition to the support in science, she has been a great mentor in diverse aspects of life. I cannot find words to express my admiration towards her.

I am especially grateful to the members of the Fenselau group (Meghan Burke, Amanda Lee, Sitara Chauhan, Lucia Geis-Asteggiant, Kate Adams, and Sara Moran) for their deep friendships and great support in both my personal and professional time at UMD. Intellectual knowledge in biochemistry provided by Meghan and Sitara has made my research richer. Amanda and Lucia have immensely helped me to learn instrumental techniques, which were fundamental for my mass spectrometry-based analysis. Especially, all the members have provided a homey environment during my graduate study. I will cherish the great memories within the Fenselau group.

The studies in this thesis were substantially enhanced by several scientists and supporting sources. I would like to thank Prof. Nathan Edwards, Georgetown University Medical Center, for his help and advice in bioinformatics. I am deeply thankful to Dr. Yan Wang, Director of Proteomic Core Facility at UMD, for her perceptive assistance in the use of MS instruments, and to Timothy Mangel, Director

of the Laboratory for Biological Ultrastructure at UMD, for his advice on transmission electron microscopy. I acknowledge Dr. Stephen Wolniak who introduced and thoroughly taught fluorescence microscopy. I am also grateful to my thesis committee members, Prof. Jason Kahn and Prof. Shuwei Li. The overall research was funded by a grant from National Institutes of Health (GM 021248). Further, I thank Republic of Korea Army for giving me the opportunity to get a graduate education.

Special thanks go to my parents, Mr. Kidong Kim and Mrs. Jeongja Sim, for their strong encouragement and support. Lastly, I would like to express my sincere gratitude to my husband, Semin, and my daughter, Hayeon, whose unconditional love and full faith made it all possible.

# Table of contents

<b>Acknowledgements .....</b>	<b>ii</b>
<b>Table of contents .....</b>	<b>iv</b>
<b>List of Tables .....</b>	<b>vii</b>
<b>List of Figures.....</b>	<b>viii</b>
<b>List of Abbreviations .....</b>	<b>xi</b>
<b>List of Appendix.....</b>	<b>xiii</b>
<b>Chapter 1: Introduction .....</b>	<b>1</b>
1.1    Bacterial EVs .....	1
1.1.1    General characteristics of bacterial extracellular vesicles (EVs).....	1
1.1.2    Functions of bacterial EVs.....	2
1.1.3    Shedding mechanisms of bacterial EVs.....	4
1.1.4    Potential of EVs in therapeutic applications .....	5
1.1.5    Gram-positive bacterial EVs.....	7
1.2    Sporulation of <i>Bacilli</i> .....	8
1.2.1    Gram-positive bacteria <i>Bacilli</i> .....	8
1.2.2    Morphological differentiation of the sporulation stages .....	10
1.2.3    Distinct biochemical events occur during sporulation.....	11
1.3    Research objectives and significance.....	13
<b>Chapter 2: Isolation and characterization of EVs shed by vegetative and sporulating <i>B. subtilis</i>.....</b>	<b>15</b>
2.1    Introduction.....	15

2.2	Materials and Methods.....	17
2.2.1	Cell cultures of vegetative and sporulating <i>B.subtilis</i> .....	17
2.2.2	EV isolation .....	18
2.2.3	Protein / lipid assays .....	18
2.2.4	Transmission electron microscopy (TEM) .....	19
2.3	Results and discussion .....	20
2.4	Summary .....	25
<b>Chapter 3: Analysis of protein cargo in EVs shed at vegetative and sporulating stages .....</b>		<b>26</b>
3.1	Introduction.....	26
3.2	Materials and Methods.....	32
3.2.1	Proteolysis.....	32
3.2.2	Peptide analysis by HPLC-MS/MS .....	33
3.2.3	Bioinformtics .....	34
3.2.4	Western blot analysis .....	35
3.2.5	Alkaline phosphatase (AP) activity assay.....	36
3.3	Results and discussion .....	36
3.3.1	Characterization of EV proteins.....	36
3.3.2	Relative abundances of proteins .....	40
3.3.3	Sporulation-associated proteins .....	47
3.4	Summary .....	53
<b>Chapter 4: Observation of interaction between <i>B. subtilis</i> cells and EVs.....</b>		<b>54</b>
4.1	Introduction.....	54



4.2	Materials and Methods.....	56
4.2.1	Deconvolution fluorescence microscopy .....	56
4.2.2	Membrane fusion assay.....	57
4.3	Results and discussion .....	58
4.4	Summary .....	61
	<b>Chapter 5: Conclusions and perspectives .....</b>	<b>62</b>
	<b>Appendix.....</b>	<b>65</b>
	<b>Bibliography .....</b>	<b>79</b>

## List of Tables

<b>Table 1.</b> List of proteins with greatest 50 $R_{SC}$ from vegetative EVs.....	41
<b>Table 2.</b> List of proteins with greatest 50 $R_{SC}$ from sporulating EVs. ....	43
<b>Table 3.</b> Enriched KEGG (Kyoto Encyclopedia of Genes and Genomes) pathways annotated in the two EV samples.....	45
<b>Table 4.</b> List of sporulation-associated proteins identified from sporulating EVs.....	47

## List of Figures

<b>Figure 1.</b> EVs isolated from <i>Bacillus subtilis</i> cells. Isolation method is described in Chapter 2. Scale bar: 100nm.....	2
<b>Figure 2.</b> Schematic drawing of the cell structure of the <i>Bacillus</i> genus. <sup>152</sup> .....	8
<b>Figure 3.</b> Thin-sectioned TEM images of (A) <i>B. subtilis</i> spore (scale bar : 100 nm) and (B) sporulating cell (scale bar : 200 nm). Imaging procedure is described in chapter 2.....	10
<b>Figure 4.</b> <i>B. subtilis</i> cell cycles and hypothetical EV biogenesis at vegetative and sporulating stages.....	13
<b>Figure 5.</b> TEM images of the isolated EVs at different growth times. EVs isolated from vegetative cultures after (A) 3 h, (B) 5 h, (C) 10 h, (D) 12 h, (E) 17 h and EVs from sporulating culture after (F) 12 h. Scale bars: 100 nm.....	20
<b>Figure 6.</b> EV diameter estimations from TEM using Image J. (A) vegetative EVs (n=200), (B) sporulating EVs (n=200). .....	23
<b>Figure 7.</b> Thin-sectioned TEM images of spores and endospore-containing cells. Endospore-containing cells with (A) a putative released EV and (B) putative EV fusing out of a cell. Free spores with unidentified (C) outer and (D) inner blebs (red arrows). Scale bars: 100 nm.....	24
<b>Figure 8.</b> Fragmentation patterns of peptides in tandem mass spectrometry. Product ions (b- and y-ions) by CID are highlighted. ....	29
<b>Figure 9.</b> Subcellular locational distributions of identified proteins based on Gene Ontology (FDR-corrected p-values $\leq 0.05$ ). The most highly assigned 10 locations	

from each EV group were selected (annotation p-value  $\leq 0.05$ ). Some proteins were located to more than one category. Unclassified proteins were not included. \*proton-transporting two-sector ATPase complex. .... 38

**Figure 10.** Molecular functional annotations of identified proteins based on Gene Ontology (FDR-corrected p-value  $\leq 0.05$ ). The most highly populated 10 functions from each EV group were selected (annotation p-value  $\leq 0.05$ ). Some proteins were located to more than one category. Unclassified proteins were not included. .... 39

**Figure 11.** Biological process annotations of proteins with  $R_{SC} > 1$  based on Gene Ontology. Biological processes of 75 proteins more abundant in vegetative EVs and 124 proteins more abundant in sporulating EVs were annotated (annotation p-values  $\leq 0.05$ ). Unclassified proteins were not included. .... 46

**Figure 12.** Western blotting of alanine dehydrogenase (stage V sporulation protein N, spoVN) in lysates of cells and EVs. (A) Western blot (8-16% SDS-PAGE) of spoVN in vegetative cell lysate (Veg.cells), sporulating cell lysate (Spo.cells), lysate of EVs from vegetative cells (Veg.EVs), and lysate of EVs from sporulating cells (Spo.EVs) with anti-spoVN polyclonal antibody. (B) Relative band intensities of spoVN blots. Intensities were determined relative to a band of positive control (purified *B. subtilis* alanine dehydrogenase) using Image J. .... 49

**Figure 13.** MS/MS spectra of sporulation-associated proteins. (A) a peptide from alanine dehydrogenase. (B) a peptide from oligopeptide transport ATP-binding protein OppD. .... 50

**Figure 14.** Alkaline phosphatase activities from EV protein cargos (n=3). .... 51

**Figure 15.** Deconvolution fluorescence microscopic images of EVs. *B. subtilis* EVs stained with (A) DiD and (B) DiO lipophilic dyes. .... 58

**Figure 16.** Deconvolution fluorescence images. (A) DAPI-stained *B. subtilis* cells (0 min incubation), (B-C) Cells incubated with DiD labeled EVs for (B) 3 min, (C) 60 min (representative images from 100-200 cells per time). DAPI labeled to chromosomes is in blue and DiD initially labeled to EVs is in red. (D) Normalized DiD fluorescence intensity on cell membranes over incubation time (Each single dot represents an average of >30 cell membranes). Intensities were measured with Image J. Scale bars: 5  $\mu\text{m}$  ..... 59

**Figure 17.** Fluorescence spectrophotometric detection of membrane fusion-like interaction between EVs and *B. subtilis* cells. (A) Fluorescence intensities of R18-labeled EVs (sporulating) following addition of cells, and subsequent disruption with Triton X100. (B) The percent of fluorescence de-quenching (FD) by the addition of cells. .... 61

## List of Abbreviations

AP	Alkaline phosphatase
ATP	Adenosine triphosphate
BHI	Brain heart infusion
CFU	Colony forming unit
CID	Collision-induced dissociation
DAPI	4',6-diamidino-2-phenylindole
DAVID	Database for Annotation, Visualization and Integrated Discovery
ESI	Eletrospray ionization
EV	Extracellular vesicles
FD	Fluorescence de-quenching
FDR	False discovery rate
GO	Gene ontology
HPLC	High Performance Liquid Chromatography
ID	Identification
IM	Inner membrane
KEGG	Kyoto Encyclopedia of Genes and Genomes
LC	Liquid chromatography
LPS	Lipopolysaccharide
LTQ	Linear trap quadrupole

MS	Mass spectrometry
MS/MS	Tandem mass spectrometry
OM	Outer membrane
OMV	Outer membrane vesicle
PBS	Phosphate buffered saline
PG	Peptidoglycan
PIR	Protein information resource
PSM	Peptide spectrum match
R18	Octadecyl Rhodamine B Chloride
R <sub>sc</sub>	Ratio of spectral count
SASP	Small acid-soluble protein
SEC	Size exclusion chromatography
TEM	Transmission electron microscopy

## List of Appendix

<b>Appendix table 1.</b> Proteins identified in vegetative EVs and sporulating EVs (distinct peptides $\geq 2$ , PSM FDR $< 5\%$ , FDR-corrected p-value $\leq 0.05$ ) .....	65
--	----



# **Chapter 1: Introduction**

## **1.1 Bacterial EVs**

### **1.1.1 General characteristics of bacterial extracellular vesicles (EVs)**

EVs are membranous and spherical vesicles shed by various eukaryotic and prokaryotic organisms.<sup>1,2</sup> They are enclosed by a lipid bilayer with nano-scaled diameters of 20 – 2000 nm depending on the organism and are released to the extracellular region.<sup>3</sup> The phenomenon of EV biogenesis is highly conserved across diverse organisms, suggesting that the EV production must have significant roles in life. Bacterial EVs were first observed from cultures of the Gram-negative bacterium *Escherichia coli* in the 1960s.<sup>4</sup> Thereafter, studies using diverse biochemical techniques have progressed extensively in both Gram-negative and Gram-positive bacteria. Gram-negative bacterial EVs (also known as outer membrane vesicles, OMVs) have been validly reported with a range from 20 to 300 nm in diameter from various species.<sup>5</sup> More recently, EVs were also found from some species of Gram-positive bacteria with similar size distributions (Figure 1).<sup>6,7</sup> As in the case with EVs of eukaryotes, bacterial EVs carry a number of cellular components, including proteins, nucleic acids, lipids, toxins, communication signals and immunomodulatory

compounds in a concentrated and protected form.<sup>8-10</sup> Biological functions of EVs have also been discussed based on the components identified.

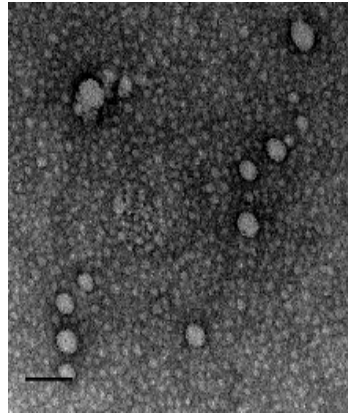


**Figure 1.** EVs isolated from *Bacillus subtilis* cells. Isolation method is described in Chapter 2. Scale bar: 100nm

### 1.1.2 Functions of bacterial EVs

Bacterial EVs have been suggested to function in numerous physiological processes and pathogenesis in host cells (in case of pathogens).<sup>1,9</sup> First of all, EVs play significant roles in bacterial intercellular communication and bacterium – host cell interactions as a novel secretion / delivery system for the biologically active components. The EV-mediated system has distinct advantages over other secretion pathways.<sup>5</sup> EVs allow components unfavorable for secretion, such as membranous proteins, bacterial lipids and hydrophobic molecules, to be efficiently secreted to the extracellular region. For instance, *P. aeruginosa* EVs have been observed to incorporate hydrophobic pseudomonas quinolone signal (PQS), which controls quorum sensing.<sup>11,12</sup> Mashburn and Whitely found that elimination of EVs significantly interrupts the cellular communication within a population and PQS-mediated group

activities.<sup>11</sup> Another benefit is that soluble proteins in EVs can be protected from extracellular hydrolytic enzymes.<sup>5</sup> Moreover, EVs deliver the functional components to distal sites in a highly concentrated form and enable targeted delivery using EV surface ligand - host receptor interactions.<sup>5,13</sup>

Secondly, EVs may contribute to bacterial survival. EVs may package intrinsic and extrinsic damaging factors and implement their release.<sup>14</sup> Accumulation of misfolded proteins and other toxic materials could attack bacterial cell surface and threaten their survival. EVs may rapidly remove these threatening components. For instance, a hypervesiculating *E. coli* mutant has been observed to have greater viability relative to a normal strain under surface-attacking conditions with either external or internal stress-inducers.<sup>14</sup> From this observation, McBroom and Kuehn proposed that efficient removal of misfolded proteins is a key feature of the stress response pathway of EVs. They also suggested that the levels of EV formation and EV contents are affected by environmental stressors.<sup>14</sup> Another proposed way by which EVs support bacterial survival is nutrient acquisition using receptors.<sup>5,12</sup> For example, PQS carried by EVs functions not only in the intercellular communication but also in acquiring nutrients.<sup>12</sup> PQS actively binds iron ( $\text{Fe}^{3+}$ ), which is crucial for bacterial survival. EVs are proposed to catch iron in the extracellular environment by forming PQS- $\text{Fe}^{3+}$  complex and deliver it to parental cells by fusion or release near the cells.<sup>12</sup> EVs can also enhance cell competitiveness by attacking other bacteria. Proteases and other lytic enzymes have been shown to be enveloped in EVs with active bacteriolytic activities.<sup>15</sup> Within EVs, these enzymes would degrade cell surfaces of either Gram-positive or -negative bacteria.<sup>15,16</sup> In addition, bacterial EVs affect bacterial survival by

involvement in nucleation, communication and stabilization of biofilms.<sup>17,18</sup> EVs have been observed to be shed from both Gram-positive and -negative bacterial biofilms.<sup>6,17</sup>

In the case of pathogenic bacteria, EVs may play a role in their pathogenicity to host cells. EVs contain toxins and other virulent factors in biologically active forms.<sup>19–</sup><sup>21</sup> These toxic materials can be delivered to host cells effectively through various mechanisms, including membrane fusion, bacterial adhesion-host receptor interaction, and endocytic uptake.<sup>22</sup> EV production can be up-regulated in infected host cells, resulting in increase of virulence and activation of immune responses.<sup>5</sup> The immunomodulatory functions of EVs will be further discussed in the topic of therapeutic applications. In addition to the direct functions, it can be assumed that EVs indirectly support pathogenic functions of bacteria by contributing to intercellular communication and bacterial survival as discussed above.

The functions reviewed here are mostly based on studies of Gram-negative EVs. Gram-positive EVs are expected to have functional similarities because of comparable components identified in Gram-negative and Gram-positive EVs.

### **1.1.3 Shedding mechanisms of bacterial EVs**

It is important to study the mechanisms of bacterial EV biogenesis in order to understand their functions and relevant biological processes. Several mechanisms have been proposed for Gram-negative bacterial OMVs, but most studies have considered disruption of interactions between outer membrane (OM) and peptidoglycan (PG) layers to be a key factor.<sup>1</sup> In general, OM and PG are stably bridged through OM-PG linking proteins and OM-PG-IM (inner membrane) linking proteins. According to the proposed mechanisms, bulging of the aOM would occur at the areas lacking the linker

proteins.<sup>1,5</sup> Another likely mechanism of OMV biogenesis is contributed by proteins gathering at specific regions of the OM inner surface.<sup>5</sup> Enrichment of periplasmic proteins would generate pressure outward, resulting in the budding of OMV. This model also requires removal of the OM-PG linkage. More recently, lipopolysaccharides (LPS) have been reported to significantly participate in OMV budding.<sup>1</sup> LPS molecules (also known as endotoxins) are critical for the architecture of the Gram-negative bacterial cell surface and trigger immune responses in host organisms. Interaction of LPS with environmental stimulants could cause the bulging of OM. Gentamicin is a popular stimulant, which is known to interact with specific LPS species on the OM based upon charge attractions.<sup>23,24</sup> This interaction would pull on the region of the OM containing the LPS species and modify the membrane curvature, inducing OMV release.<sup>25</sup> The cell envelope structure of Gram-positive bacteria is substantially different from that of Gram-negative bacteria. The Gram-positive bacterial cell has a single layer of membrane, which is covered by a thick layer of peptidoglycan. Due to the structural difference, shedding mechanisms of Gram-positive bacterial EVs are expected to be unlike those of Gram-negative bacteria. Further analysis of the mechanisms for both types of bacterial EVs are needed.

#### **1.1.4 Potential of EVs in therapeutic applications**

As discussed in the previous section, EVs may carry virulent factors and activate immunity in host cells.<sup>22</sup> Furthermore, they have shown high efficiencies of internalization into host cells and are susceptible to biochemical manipulations including genetic recombination of parental cells.<sup>22,26,27</sup> With these characteristics, EVs are considered to be attractive candidates for vaccines against pathogenic bacteria.<sup>27</sup>

Clinical trials of immunization using bacterial EVs are rapidly emerging and some natural Gram-negative bacterial EVs have already been licensed as vaccine platforms.<sup>28-30</sup> The attempt to develop vaccines using EVs initially started for serogroup B meningococcal disease induced by Gram-negative bacterium *Neisseria meningitidis*. The natural EVs from *N. meningitidis* have been successfully applied for epidemic control in Cuba, Norway, Chile, Brazil and New Zealand.<sup>30</sup> Until now, the protein-based EV-vaccines are the only formulations that provide sufficient immunogenicity against the serogroup B meningococcal disease.<sup>30</sup> In addition to the native forms, EVs have been genetically or physically modified in order to increase their efficacy for immunization and facilitate administration.<sup>26,27</sup> During production and purification steps, the properties of EVs can be chemically and physically altered by mechanical shearing, and treatments with detergents or other chemicals.<sup>27</sup> Detergent-assisted EV extraction is the most popular treatment and known to produce higher yields with reduced toxicity from LPS. Considering these benefits, the detergent-treatment is considered to be necessary for EV-vaccines against the serogroup B meningococcal disease. However, this approach has also been found to decrease immunogenicity and promote aggregation.<sup>26</sup> In order to overcome these side-effects, genetic manipulations designed for toxicity attenuation and for increase of the EV yield have been implemented without detergent treatment.<sup>26</sup> Further, diverse techniques to induce and enhance shedding of EVs have been employed, including induction of autolysis, inhibition of protein synthesis, and treatment with gentamycin.<sup>27</sup> The development of EV-based vaccines for diverse Gram-negative pathogenic bacteria

is in progress, however development for Gram-positive bacterial infections has not started yet.

### **1.1.5 Gram-positive bacterial EVs**

Originally, Gram-positive bacteria were considered not to shed EVs, since they lack outer membranes, but in 1990 EVs were observed microscopically from Gram-positive bacteria.<sup>31</sup> Subsequently, Gram-positive bacterial EVs from *Staphylococcus aureus*, *B. anthracis*, *B. subtilis*, *Streptomyces coelicolor*, *Listeria monocytogenes*, *Clostridium perfringens*, and *Streptococcus pneumoniae* have been isolated and characterized.<sup>6,7,21,32–35</sup> Proteomic profiling of Gram-positive bacterial EVs was initially reported by Lee *et al.* for *S. aureus*.<sup>7</sup> The proteome of EVs shed by *S. aureus* was found to contain proteins with similar functional annotations to those of OMVs from Gram-negative bacteria, including proteins involved in immunity, pathogenesis, and drug response.<sup>7,32,34</sup> EVs of *B. anthracis* were reported to carry toxin components and, more importantly, be capable of immunization.<sup>21</sup> In the study of *B. subtilis*, EVs were shown to be shed directly from cells, not from lipid aggregations and be disrupted by lipopeptide surfactin.<sup>6</sup>

Characterization of EVs from Gram-positive bacteria is still at an early stage, while Gram-negative bacterial EVs have already been evaluated for antibiotic or vaccine development. Further investigation of the biogenesis mechanisms and biological activities of Gram-positive bacterial EVs are required for therapeutic applications and for better knowledge of bacterial physiology.

## 1.2 Sporulation of *Bacilli*

### 1.2.1 Gram-positive bacteria *Bacilli*

The genus *Bacilli* are aerobic (or anaerobic under some conditions), rod-shaped and endospore-forming Gram-positive bacteria, which are widely found in soil and water. This genus was initially defined by Ferdinand Cohn in the 1870s.<sup>36</sup> The *Bacillus* cell is typically composed of cytoplasm (including nucleoid and ribosomes), cell membrane, cell wall and flagella (Figure 2). Based on taxonomic criteria, *Bacillus* has been considered as the most heterogeneous genus with more than 80 solidly described species.<sup>37</sup> In spite of the heterogeneity, *Bacilli* can be characterized by their morphology and simple biochemical analysis, such as test of color photomicrographs,<sup>38</sup> chromatographic analysis of fatty acid methyl esters,<sup>39</sup> and 16S rDNA sequencing assay.<sup>40</sup> The two important aspects of the genus *Bacillus* are endospore formation and

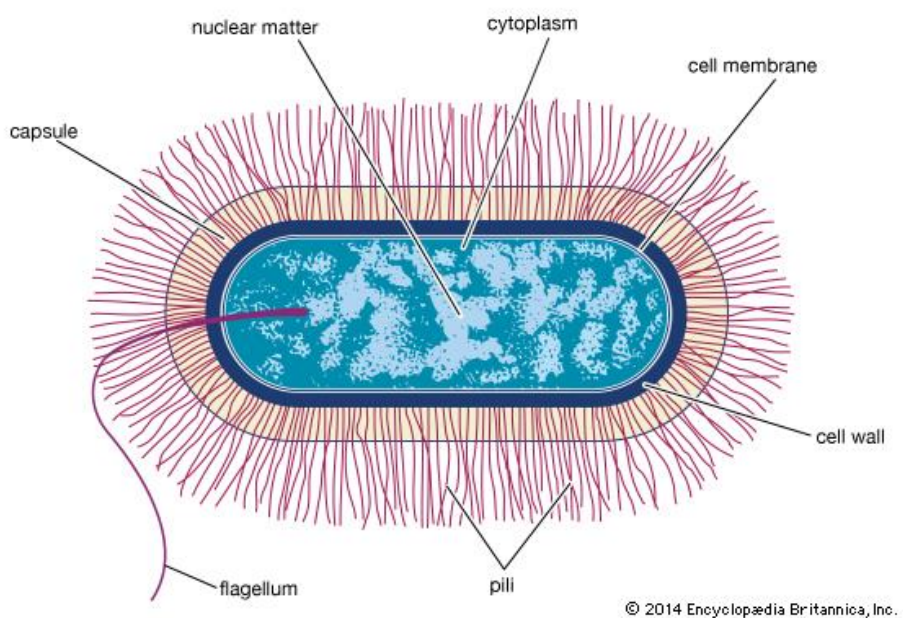


**Figure 2.** Schematic drawing of the cell structure of the *Bacillus* genus.<sup>152</sup>



pathogenic components (restricted to some species). The most familiar pathogenic species is *B. anthracis*, which carries three exotoxin components named: protective antigen, edema factor, and lethal factor.<sup>42,43</sup> *B. anthracis* can deliver the toxins with high stability by forming spores, and thus the spores have been utilized for bioterrorism.

*Bacillus subtilis* is the most extensively analyzed species among *Bacilli*. It was initially named *Vibrio subtilis* by Christian Gottfried Ehrenberg and renamed *Bacillus subtilis* by Cohn.<sup>36</sup> Since then, several hundred *B. subtilis* strains have been found.<sup>41</sup> This species is readily found in soil and has been observed in normal gut commensal in human.<sup>44</sup> A single cell of *B. subtilis* has numerous flagella, which provide efficient swarming mobility in liquids.<sup>45</sup> Since it is highly amenable to genetic manipulation, *B. subtilis* is the most widely investigated Gram-positive bacterium and has served as a paradigm for various biochemical studies of bacteria, especially for analysis of sporulation.<sup>46</sup> It seems appropriate to examine EVs shed by *B. subtilis* to establish basic understanding of the proteins in EVs from Gram-positive bacteria.

### 1.2.2 Morphological differentiation of the sporulation stages

Sporulation is a cell developmental process of Gram-positive bacteria that are responding to nutrition exhaustion. This distinct process has been regarded as a simple model of cellular differentiation.<sup>47</sup> The formation of the endospore was first observed in *B. subtilis* and *B. anthracis*.<sup>41</sup> The spore is structurally composed of spore core, membranes, cortex, spore coats, and (in some species) exosporium (Figure 3).<sup>48</sup> The series of sporulation stages is typically classified based on distinct morphological changes (Figure 4).<sup>49</sup> First, cells at the sporulation stage 0 are ordinarily growing under vegetative condition. Stage I designates the point at which a single axial chromatin filament is formed, while the cell at stage II produces an asymmetric septum at a pole of the cell. Stage II is often considered as the actual starting point of sporulation. As the asymmetric septum is completed, the smaller compartment, called a forespore, is engulfed by the larger compartment, termed a mother cell, which is a transition from stage II to stage III. Next, at stage III, the forespore becomes a free protoplast with two layers of cytoplasmic membranes in the mother cell. In the subsequent stage IV, cell

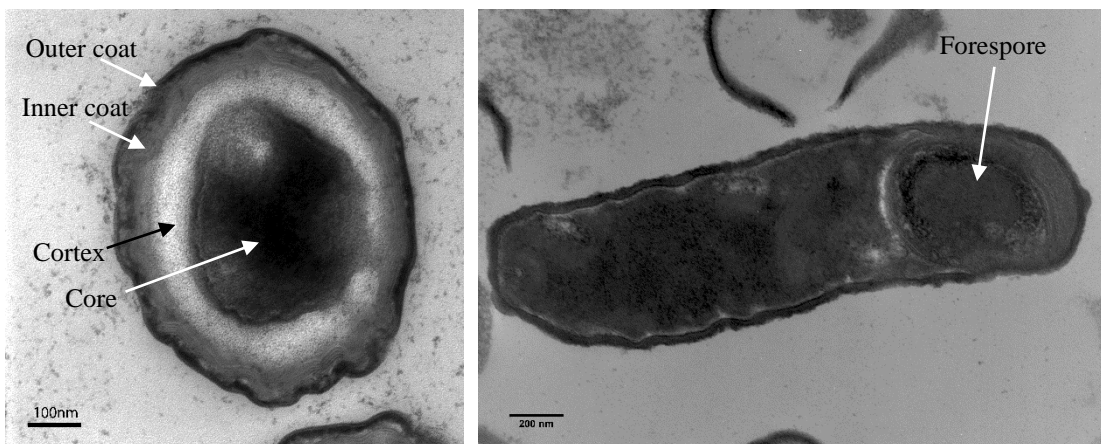


**Figure 3.** Thin-sectioned TEM images of (A) *B. subtilis* spore (scale bar : 100 nm) and (B) sporulating cell (scale bar : 200 nm). Imaging procedure is described in chapter 2.

wall and cortex surround the forespore, followed by stage V in which spore coat proteins accumulate on the outer surface of the endospore. Eventually, the spore matures during stage VI and the mother cell lyses and releases the free spore in stage VII. The released spore becomes dormant and survive for a long time and under harsh conditions. They also can proceed to germination and reform vegetative cells under suitable environments.

### **1.2.3 Distinct biochemical events occur during sporulation**

A number of biochemical events specific to sporulation have been analyzed and used to characterize sporulation stages. These events have distinct correlations with the morphological stages and result in synthesis of stage-specific proteins and other products. In the early stages 0-II of sporulation, the cells increase production of diverse enzymes including  $\alpha$ -amylase, proteases, and nucleases. Alkaline phosphatase and extracellular deoxyribonuclease are known as stage II markers.<sup>50</sup> During the subsequent stages, other components important for spore maturation and their viability are expressed either in the forespore, in the mother cell, or at the interface between the mother cell and the forespore.<sup>49</sup> Specifically at stage III,  $\beta$ -galactosidase and glucose dehydrogenase are highly enriched and thus they have been used for the stage screening as marker proteins characteristic of stage III.<sup>50</sup> The forespores also synthesize a group of small acid-soluble proteins (SASPs) mostly during stage III, which contribute to the UV-resistance of spores. Importantly, each species of *Bacillus* group bacteria has species-specific sequences of SASPs, which can be used for species identification.<sup>51</sup> In stages IV and V, the mother cell provides spore coat proteins, while the cell wall and cortex are made in the intermembrane space between the mother cell and forespore.

The multiple layers covering the spore allow it to maintain stability in harsh environments.<sup>49</sup> Lastly, dipicolinic acid produced at the last stage of spore maturation plays a significant role in protecting spores, especially spore DNA.<sup>52</sup> These stage-specific products have been used to determine sporulation stages.<sup>53-57</sup>

In addition to the synthesis of specific enzymes and metabolites during sporulation, another noteworthy aspect of spores is substantially high resistance to numerous biochemical and physical stressors, including chemicals, heat, UV radiation, mechanical disruption and so forth.<sup>48,50</sup> Determination of the spore resistance to these environmental stressors can distinguish spores from vegetative cells<sup>58-60</sup>. With such resistance, *Bacillus* spores can endure for a long time period and be an effective means of transport for toxic components.<sup>47,61</sup>

### 1.3 Research objectives and significance

Based on the knowledge of two important biological processes—sporulation and EV biogenesis—I aim to examine possible correlations between these processes. Under this main goal, the first sub-objective is to confirm the production of EVs at diverse growth stages of *B. subtilis*, especially during sporulation. It is a significant step because EVs from sporulating cells have not been reported. In this step, a specific isolation technique and high-resolution microscopy are required to accommodate the nano-scale size of the EVs. After verifying the presence of EVs, my second sub-objective is to optimize the cell preparation and EV isolation procedures from vegetative and sporulating phases to obtain optimal and comparable amounts of EVs.

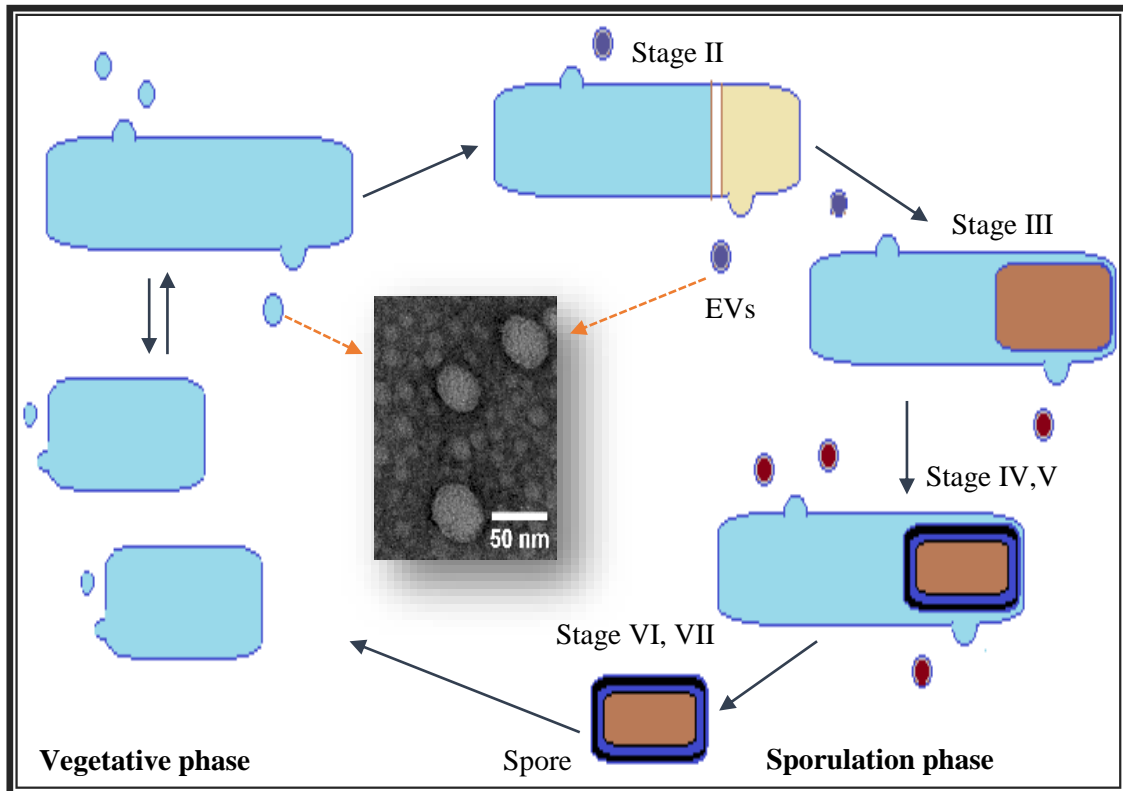


**Figure 4.** *B. subtilis* cell cycles and hypothetical EV biogenesis at vegetative and sporulating stages

With the EVs collected from vegetative and sporulating cells, my third sub-objective is to quantitatively compare the proteomes of EVs produced at the two different stages using tandem MS and bioinformatics techniques. The protein profiling may suggest natural functions of bacterial EV. Additional characterizations of EV proteins have been performed by enzymatic assay and western blotting in order to support MS-based analysis. My last sub-objective is to observe interaction between EVs and *B. subtilis* cells. Observation of their communication would provide evidence for the transfer mechanisms of EV contents into bacterial cells.

Unlike Gram-negative bacterial EVs, little is known about Gram-positive bacterial EVs. Foundational knowledge is vitally needed. In this study, Gram-positive bacterium *B. subtilis* is used, for which there is the most extensive genomic and proteomic information. This study on the relationship between EV production and sporulation is expected to enhance understanding of *B. subtilis* biology and accelerate analysis on various Gram-positive bacterial EVs.

# **Chapter 2: Isolation and characterization of EVs shed by vegetative and sporulating *B. subtilis***

## **2.1 Introduction**

Gram-negative bacterial OMV production has been observed under a wide range of growth stages and conditions including in liquid media,<sup>9,13</sup> agar plates,<sup>62</sup> in biofilms<sup>17</sup>, within eukaryotic hosts<sup>63,64</sup> and even during bacteriophage infection.<sup>65</sup> Moreover, OMV biogenesis has been found to be stimulated by environmental changes such as nutrient depletion<sup>66</sup> and treatment with antibiotics.<sup>67</sup> Gram-positive bacteria were also reported to shed EVs into liquid media during exponential growth phase, stationary phase, and in biofilms,<sup>6,7,21</sup> but not after death.<sup>6</sup> However, the effect of collecting time points on EV production for has not yet received attention. In addition, it is still not known whether EVs are produced even during sporulation.

The most popular technique for isolating bacterial EVs is differential ultracentrifugation supported by membrane filtration.<sup>68</sup> Centrifugation at relatively low speed ( $\leq 15,000 \times g$ ) removes cells and cell debris, followed by spinning at high speed ( $\geq 50,000 \times g$ ) to pellet the EVs for the last centrifugation step. In addition to the speed, diverse other factors such as distance from rotation axis, rotor type, and viscosity of solution have decisive effects on the size, homogeneity, purity, yield, and membrane integrity of vesicles.<sup>69</sup> Thus, one need to take account of these factors for optimizing the isolation method. After low speed centrifugations, supernatant is often filtered

through 0.22-0.45 $\mu$ m filtering devices in order to minimize remaining contaminants.<sup>70,71</sup> Density gradient centrifugation using sucrose or Oerptiprep<sup>TM</sup> for 16 – 20 hours may follow the last pelleting step for more stringent purification.<sup>72</sup> However, the adequate centrifugation time is still uncertain. With inadequate time, some EVs may not be deposited in a density fraction for EVs, while contaminants may stay in the same density fraction as EVs.<sup>69</sup>

Size exclusion chromatography (SEC) has recently emerged as an efficient alternative method that provides EVs of relatively homogeneous size with high purity.<sup>27</sup> This method is considered ideal for therapeutic applications of bacterial EVs, in which purity is critical.<sup>73</sup> A simplified single-step isolation method using SEC has been also proposed.<sup>74</sup> However, chromatographic separation may decrease the yield of EVs because of the dilution into several fractions and non-specific interaction with the column beads.<sup>75</sup>

Morphological characterization of purified EVs is indispensable in order to confirm the presence and purity of isolated EVs. For this step, microscopic techniques with high resolution are required because of the nano-scale size of EVs. Transmission or scanning electron microscopy is commonly chosen and, rarely, atomic force microscopy can be also applied for 3 dimensional profiling.<sup>76</sup> Further, electron microscopy with embedding technique has been used to detect shedding and fusion events of EVs from a cell.<sup>6,15</sup>

In this chapter, EVs were isolated at the stationary phase and the sporulating phase separately in order to observe the production of EVs across those developmental stages. Procedures of cell growth and EV isolation were optimized for *B. subtilis* at



vegetative and sporulating phases based on the differential ultracentrifugation method. The collected EVs were further characterized by negative staining TEM, protein and lipid assays.

## **2.2 Materials and Methods**

### **2.2.1 Cell cultures of vegetative and sporulating *B. subtilis***

*B. subtilis* 168 (Ind<sup>-</sup>, Tyr<sup>+</sup>, ATCC #23857, Manassas, VA) cells from freeze-dried stock were plated on brain heart infusion of 37 g in 1 L distilled water (BHI, Becton Dickinson, Franklin Lakes, NJ) with 1.5% agar. All cell cultures were produced at 37°C. For vegetative growth, a single colony was transferred to 5 mL of BHI broth (37 g BHI in 1 L distilled water) for sub-culture. Cells from the sub-culture were incubated in 500 mL BHI broth for 12 h, unless noted otherwise, and centrifuged at 10,733 ×g for 25 min at 4°C. The cell pellet was resuspended in Dulbecco's phosphate buffered saline (PBS) and pelleted at the same centrifugation as described above. The washed cells were resuspended in BHI-based sporulation medium and subsequently incubated for 12 h. BHI-based sporulation medium was produced by modifying SM resuspension medium.<sup>77</sup> Briefly, this medium consists of 6 g BHI (~32% of normal BHI broth), 12 mg MnCl<sub>2</sub>, 4.8 g MgSO<sub>4</sub>, and 0.2 g CaCl<sub>2</sub> in 500 mL water. The cells grown in sporulation medium were pelleted and washed as done for the vegetative cells. The supernatants from vegetative and sporulating cultures were subject to EV isolation, separately. Three biological replicates were prepared for cells and EVs at vegetative and sporulating conditions. Colony forming units for each replicate were measured

using serial dilutions. The production of spores was detected using Schaeffer-Fulton staining phase contrast microscopy.<sup>78</sup>

### **2.2.2 EV isolation**

EVs were collected from vegetative and sporulating cell cultures according to published methods<sup>7,21</sup> for Gram-positive bacterial EVs, with slight modifications. Briefly, the collected supernatants from cell cultures were filtered using a 0.22  $\mu\text{m}$  bottle-top vacuum filter (Corning, Tewksbury, MA) to remove remaining cell debris. EVs were pelleted by ultracentrifugation for 90 min at 150,000  $\times g$  at 4°C and the resulting pellet was washed with PBS at the same condition of ultracentrifugation (Optima™ LE-80K ultracentrifuge with 70Ti™ rotor, Beckman Coulter, Indianapolis, IN). Each pellet was resuspended in PBS. Lastly, the isolated EVs were washed with PBS through a 100 kDa Amicon filter three times. The isolated EVs were stored in PBS at -80°C until further use.

### **2.2.3 Protein / lipid assays**

Protein concentrations of purified EVs were determined using a Pierce BCA protein assay kit (Thermo Fisher Scientific, Rockford, IL) according to the user manual. An aliquot of EVs was incubated with 5 $\mu\text{M}$  DiO lipophilic dye (Invitrogen, Grand Island, NY) in PBS for 1 h at room temperature in order to estimate lipid contents of EVs. Amounts of vesicular lipids were measured using F-4500 fluorescence spectrophotometer (Hitachi, Tokyo, Japan). Excitation wavelength was fixed at 498 nm and emission fluorescence intensity was measured at 510 nm. The total intensities of unstained EVs and free dye solution were used for background subtraction.<sup>79</sup>

## 2.2.4 Transmission electron microscopy (TEM)

Negative staining TEM was used in order to analyze the presence and purity of isolated EVs. Bacitracin (1%) was applied on a carbon-coated formvar grid to spread vesicles. Tenfold diluted EV solutions were added on the grid and washed three times by double-distilled water. The EV samples on the grids were strained with 2% uranyl acetate for 30 sec. Images of EVs were captured at an accelerating voltage of 80 keV on a Zeiss EM10CA TEM (LEO Electron Microscopy, Thornwood, NY).

For the thin-sectioning TEM, sporulating cells prepared as described above were primarily fixed with 2% glutaraldehyde for 1 h at room temperature followed by 12 h at 4°C and they were additionally washed with PBS by three cycles of resuspension, followed by centrifugation at 10,000 x g at room temperature. For secondary fixation, the pellet was then resuspended and incubated in 1% OsO<sub>4</sub> in cacodylate buffer for 1 h and excess OsO<sub>4</sub> was removed by washing with double-distilled water three times as in the above PBS washing steps. The cells were then stained with 2% uranyl acetate for 1 h and pelleted. The pellets were dehydrated in a serial ethanol solutions of 35, 50, 70, 95 and three changes of 100% for 10 min per each concentration. After dehydration, the samples were embedded in Spurr's resin and polymerized at 70°C for 10 h<sup>80</sup>. Thin sections were obtained using a Reichert Ultracut E ultramicrotome with a diamond knife (Leica, Vienna, Austria) and placed on carbon-coated formvar grids. The sections were post-stained with 0.2% lead citrate and 2% uranyl acetate and examined on TEM.<sup>81</sup>

## 2.3 Results and discussion

*B. subtilis* 168 cells were grown in BHI liquid medium under vegetative growth for 3, 5, 10, 12, and 17 hours. EVs were collected from the cells at each time point in order to find optimal collecting time for adequate amount of EVs at vegetative growth phase. The cells were in exponential growth phase at 3 h, while they were in stationary phase at 5, 10, 12, and 17 h. EVs were detected at all time points by negative staining TEM (Figure 5).

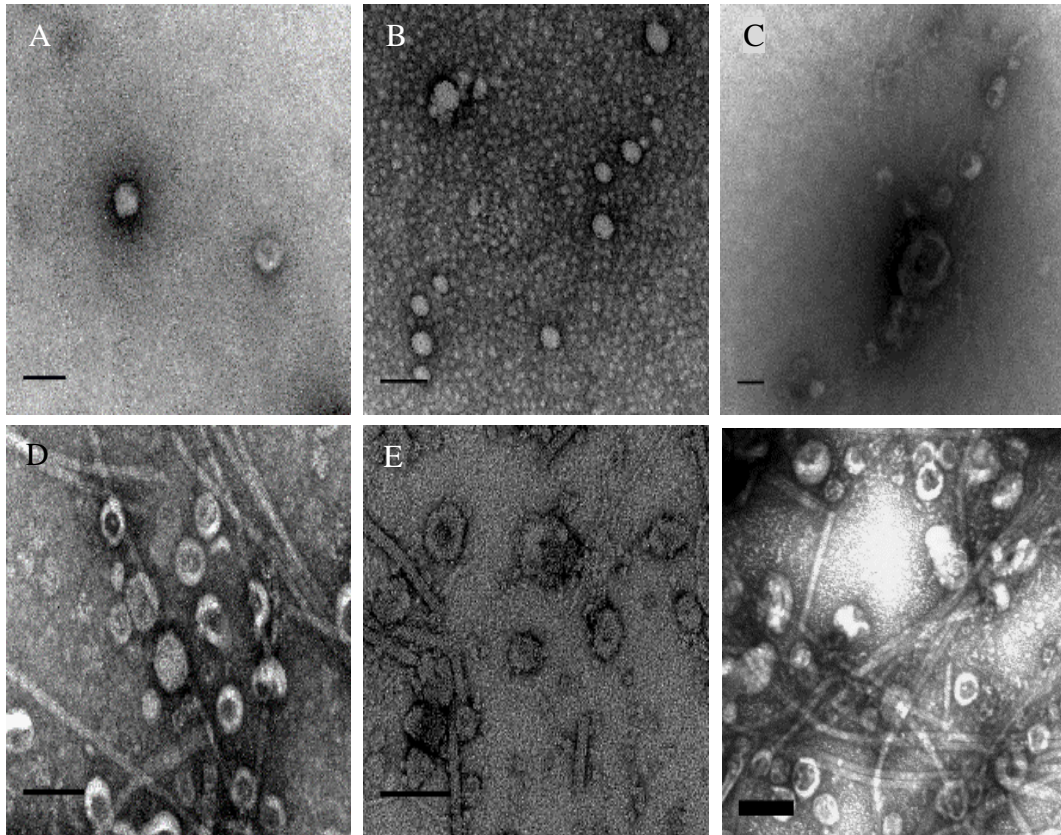


**Figure 5.** TEM images of the isolated EVs at different growth times. EVs isolated from vegetative cultures after (A) 3 h, (B) 5 h, (C) 10 h, (D) 12 h, (E) 17 h and EVs from sporulating culture after (F) 12 h. Scale bars: 100 nm.

The pellet of EVs from *B. subtilis* 168 has been observed to be brownish.<sup>6</sup> In this study, the resulting pellets from 3 and 5 h cultures were translucent while those from 10, 12 and 17 h cultures were brownish. Growth time of 12 h was selected because the amounts of EVs from 3 and 5 h cultures were inadequate for proteomic analysis and some cells from 17 h culture were observed to have already started sporulation based on phase contrast microscopy. Also, a growth time of 12 h has been previously reported to be optimal for EV isolation from *B. subtilis*.<sup>6</sup> In order to collect EVs from sporulating cells, the cells grown for 12 h in BHI medium were washed and additionally grown in BHI-based sporulating medium for 12 h. The amount of cells grown in vegetative medium for 12 h was  $[2.9 \pm 0.1] \times 10^7$  CFU/mL (n=3) and the cells additionally grown in sporulating medium for 12 h was  $[3.1 \pm 0.4] \times 10^8$  CFU/mL (n=3). The higher CFU in sporulating culture is presumably due to continuous growth of some cells and germination of some spores. An alternative cell counting method using hemocytometer resulted in significant uncertainty because of non-specific shapes of endospore-forming cells. Thus, more reliable cell counting methods may be needed to obtain an absolute comparison between the amounts of cells in the vegetative and the sporulating media.

The EV isolation method was slightly modified from previous publications.<sup>6,7,21</sup> A minimum ultracentrifugation time at the input speed is reported to be 1 h for EV isolation.<sup>82</sup> However, the stability of EVs decreases as the isolation time increases. Considering both factors, an ultracentrifugation time of 90 min was selected. After an initial washing step by ultracentrifugation, EVs were additionally washed by buffer changes through a 100 kDa filter. The EV isolation method optimized for vegetative

cell culture was also applied to the sporulating cell culture grown in BHI-based liquid sporulating medium. The resulting pellet at the ultracentrifugation step was also brownish. Relative intensities of EV lipid contents were detected by labeling EVs with DiO lipophilic dyes in order to estimate the amount of EVs produced by comparable numbers of vegetative and sporulating *B. subtilis*. The lipid contents of EVs were determined as  $[6.7 \pm 0.1] \times 10^{-7}$  (DiO intensity/CFU, n=3) at vegetative phase and  $[1.3 \pm 0.4] \times 10^{-7}$  (DiO intensity/CFU, n=3) at sporulating phase. Vegetative cells showed higher EV production than sporulating cells. However, lipid contents per cells were possibly underestimated because sporulating cells have a chance to be germinated during CFU measurement.

The presence and purity of EVs collected at several time points during vegetative growth and sporulation were examined by negative staining TEM (Figure 5). Although the amount of EVs seen varied, EVs were detected across a broad range of cell growth time including the sporulating phase. In order to evaluate size distributions of vegetative EVs and sporulating EVs, Image J was used to estimate diameters of EVs in TEM images of 200 EVs from the 12 h vegetative culture and 200 EVs from the 12 h sporulating culture.<sup>83</sup> Both populations were distributed mostly between 30 and 150nm and centered at 60nm (Figure 6). The size distributions of two EV groups were similar to each other. Diameter measurement from TEM images has been proposed to underestimate the size relative to other hydrodynamic measurements.<sup>6,84,85</sup> Other microscopic techniques such as cryo-EM may be applied if more absolute estimation of EV diameter is required.<sup>69</sup>

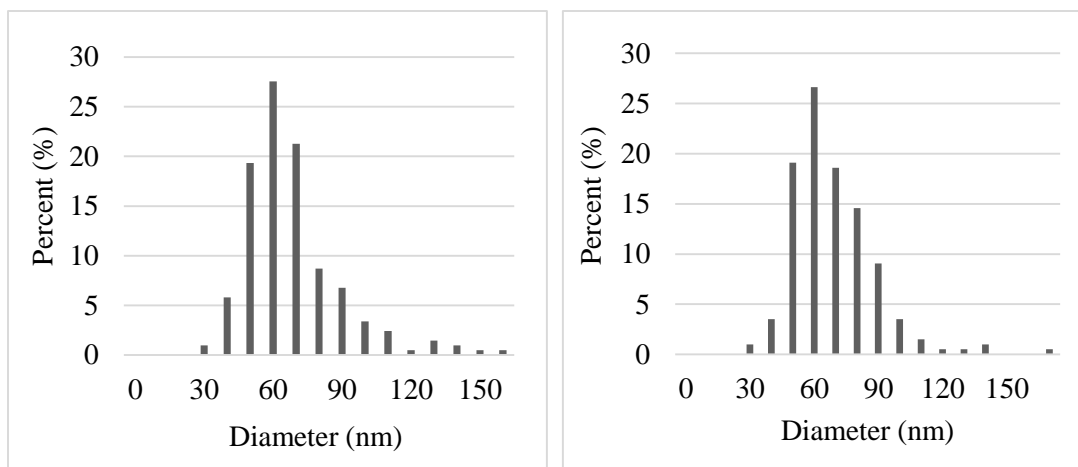


**Figure 6.** EV diameter estimations from TEM using Image J. (A) vegetative EVs (n=200), (B) sporulating EVs (n=200).

As reported by others,<sup>6,32</sup> some flagella were observed in TEM images with both vegetative and sporulating EV populations. *B.subtilis* is known to have highly enriched flagella on the cell surface, and it is difficult to avoid co-isolating flagella with EVs. Less flagella were detected from the cells harvested at shorter growth times, but the amount of EVs was also reduced. Density gradient ultracentrifugation is often used for further purification. However, flagella have been observed to remain after the density gradient step.<sup>6</sup> Even after the density gradient step, flagella have been identified either by TEM or by MS-based proteomics. In the proteomic study flagella-associated proteins are discarded.

With the detection of EVs from sporulating *B.subtilis* culture, we speculated that EVs may come from either the sporulating cell membrane or the premature endospore membrane in the mother cell. In order to capture the event of EV release, sporulating cells and free spores were examined by thin-sectioning TEM (figure 7).

Some unidentified extracellular blebs in a range of EV sizes were detected from sporulating cells (figure 7A, B), but the images were not sufficiently clear to confirm the shedding event of EVs. It is possible that EVs blebbing out from the cells might be disrupted during the sample preparation for thin-sectioning TEM. Putative extracellular and intracellular blebs were also observed from free spores released from mother cells (figure 7C, D) However, mature spores have a weak likelihood to shed EVs because the released free spores are firmly covered by cortex, spore coats and exosporium over

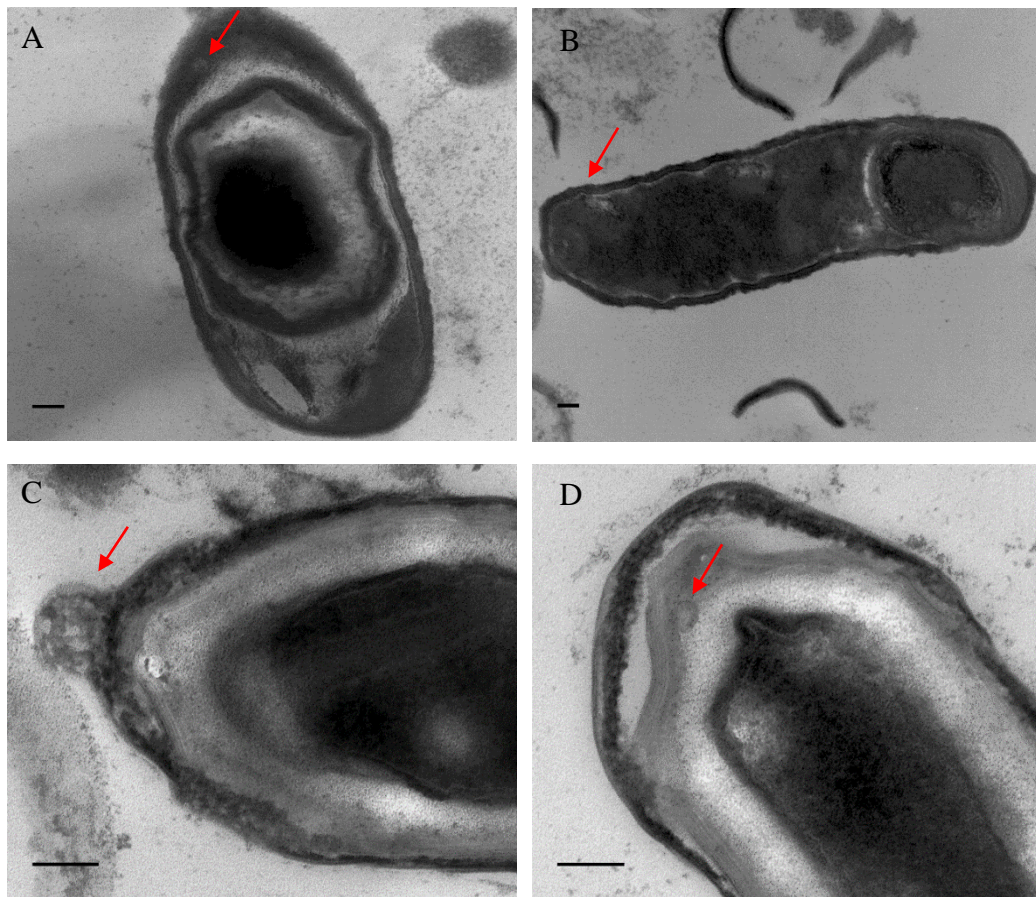


**Figure 7.** Thin-sectioned TEM images of spores and endospore-containing cells. Endospore-containing cells with (A) a putative released EV and (B) putative EV fusing out of a cell. Free spores with unidentified (C) outer and (D) inner blebs (red arrows). Scale bars: 100 nm



the spore membrane. Better techniques for thin-sectioning sample preparation and TEM examination would answer the question whether EVs are also shed from the prespore in a cell.

## 2.4 Summary

In this chapter, the EV isolation method was optimized and the isolated EVs were microscopically characterized. *B. subtilis* cells were observed to shed EVs at several different stages including the sporulation phase with size distributions that fall within the range proposed from other bacterial species.<sup>86</sup> These observations suggest that EV biogenesis is a continuous and universal process over the broad cellular life span of *B. subtilis*. Also, EV production can be assumed to be a highly conserved biological phenomenon in bacteria. The relative amount of EVs produced from sporulating cells was comparable with that from vegetative cells, which indicates that the cells are actively shedding EVs even during sporulation.

Due to technical limitations, contamination with flagella occurred in all EV extracts and the shedding event of EVs from a cell was not clearly detected by TEM. Improvement of methods for these issues may be implemented using alternative techniques such as SEC for the isolation step and Cryo-EM for the microscopic characterization.

## **Chapter 3: Analysis of protein cargo in EVs shed at vegetative and sporulating stages**

### **3.1 Introduction**

Since *B. subtilis* cells naturally produce EVs across diverse cellular growth stages, EVs are expected to have biological significance. Tandem MS-based proteomics is an indispensable technique to understand diverse aspects of EVs including their functions and biological processes in which EV proteins are involved.

Proteomics refers to the large-scale study of proteins, covering structural information, cellular functions, variations, modifications of the proteins and quantitation. Although various techniques contribute to proteomics, such as electrophoresis, microarray and microscopic imaging, current proteomic analysis mostly relies on MS.<sup>87,88</sup> MS analyzes both small and large molecules measuring the mass-to-charge ratio ( $m/z$ ) of ionized samples. Importantly, the analytes are required to be ionized and transferred into the gas-phase for mass spectrometric measurements. MS instrumentation includes an ion source, a mass analyzer and a detector. Instrumentation settings can be optimized depending on characteristics of each analysis, and they affect the results significantly. Especially, it is important to determine evaluation parameters such as resolution, mass accuracy, and sensitivity in the mass analyzer.<sup>89</sup> Ion trap (including linear ion trap and orbitrap), time-of-flight, quadrupole, and Fourier transform ion cyclotron are the basic types of mass analyzers. Each

analyzer performs the  $m/z$  in a distinctive way. Tandem MS combines two or more mass analyzers and is often used in combination with a separation tool. The tandem MS instrumentation of choice in this study was hybrid ion trap-orbitrap (LTQ-orbitrap XL<sup>TM</sup>, San Jose, CA) with electrospray (or nanospray) ionization (ESI). ESI is a ‘soft’ ionization technique that produces ions in the gas-phase without fragmentation.<sup>90</sup> In the system, highly charged droplets are sprayed under an electric field and ions are converted into the gas phase as the solvent is evaporated. This method is the most compatible interface for LC-MS and extends the mass range of the analyzer with multiple charges.<sup>91</sup>

The LTQ-Orbitrap hybrid mass spectrometer is a combination of a linear ion trap and an Orbitrap mass analyzer.<sup>92</sup> The LTQ is a 2-dimensional quadrupole ion trap, which is constructed with 4 rods and uses oscillating direct current and radio frequency potentials.<sup>89,93</sup> In the LTQ, the trapped ions in a specific  $m/z$  range are ejected using a mass selective instability operation.<sup>93,94</sup> The LTQ has advantages in ion trapping efficiency, ion-storage capacity, ion-ejecting efficiency, scan speeds, and detection sensitivity compared to 3-D ion trap.<sup>93</sup> The Orbitrap is also an ion trap mass analyzer consisting of a central spindle-like electrode and a coaxial barrel-like outer electrode.<sup>95</sup> The orbital trapping of ions occurs around the central spindle-like electrode with an electrostatic field. The trapped ions undergo harmonic oscillations and the frequencies of the oscillations are dependent on  $m/z$  values. The ion frequencies are acquired by the image current and converted to mass spectra by fast Fourier transform. The orbitrap has significant enhancements in mass resolution, mass accuracy, dynamic range, and sensitivity relative to other trap instruments.<sup>95</sup>

Three major approaches for MS-based proteomics are top-down, middle-down, and bottom-up. The top-down approach analyzes intact proteins without digestion, while the middle-down identifies relatively large peptides in a range of 3-20kDa, and the bottom-up processes small peptides produced by practically complete enzymatic or chemical cleavages.<sup>96</sup> Among these methods, the bottom-up approach has mostly been used for global profiling of proteins or proteomes from complex mixtures.<sup>97</sup> When coupled with high-performance liquid chromatography (HPLC), the bottom-up approach has higher separation efficiency and better sensitivity compared to the others.<sup>88,97,98</sup>

In a common workflow of MS-based bottom-up proteomics, biological samples of protein mixtures are digested to peptides either by enzymatic or by chemical means. Enzymatic digestion by trypsin is the most widely used method. The peptide mixtures are separated generally by one or multiple dimensional separation techniques, including electrophoresis and/or chromatography. Among various separation techniques, LC has advantages in efficiency of a continuous separation for numerous proteins, and compatibility with MS.<sup>88</sup> In the subsequent MS analysis, peptide fractions are ionized by ESI system and analyzed by tandem mass analyzers. The first stage of mass analysis scans precursor ions and provides mass to charge ratios of injected peptides or proteins (MS1). Precursor ions of interest are selected to be fragmented. After fragmentation, product ions are formed by bond cleavages and scanned in the second mass analyzing system (MS2). Types of product ions vary depending on fragmentation methods (Figure 8). The most common fragmentation technique is collision induced dissociation (CID), in which precursor ions collide with inert gas such

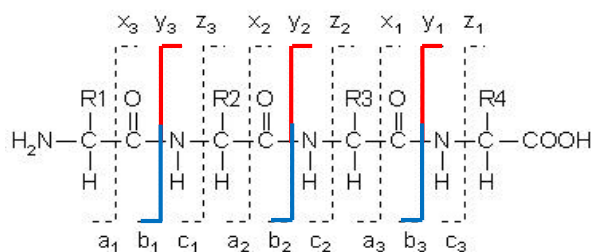


**Figure 8.** Fragmentation patterns of peptides in tandem mass spectrometry. Product ions (b- and y-ions) by CID are highlighted.

as helium or nitrogen,<sup>99</sup> resulting in peptide backbone cleavages mostly at the peptide bonds.

The resulting mass spectra are processed to identify peptides and proteins. The MS1 and MS2 spectra of a peptide mixture contain massive amount of information, which needs to be analyzed by computational techniques. The raw mass spectra are first converted to data processing formats, which are then searched against protein sequence database. Search algorithms match the experimental tandem mass spectra with theoretical MS2 spectra, which are generated from a list of possible peptide sequences and their fragments based on a selected database. There are diverse automated database searching engines such as MASCOT,<sup>103</sup> SEQUEST,<sup>104</sup> X!Tandem,<sup>105</sup> and PepArML.<sup>106</sup> More recently, new types of search engines that match observed spectra with consensus spectra based on previous identifications have also emerged and been reported to improve searching efficiency and accuracy.<sup>107,108</sup> All types of search engines score the searched peptides and then report top-scoring peptides, which are referred to peptide-spectrum matches (PSMs).<sup>107</sup>

The selection of a database affects peptide identifications considerably, because assignment of peptides is limited to sequences in the database.<sup>100</sup> UniProt/SwissProt,<sup>101</sup>

RefSeq,<sup>102</sup> and UniProt/TrEMBL<sup>101</sup> are popular examples of databases. UniProt/SwissProt and RefWeq are well-curated sequence databases based on experimental evidence, while TrEMBL contains sequences translated from genomic database or from proteins submitted to UniProt/SwissProt but not yet curated. The translated and uncurated databases provide a large number of sequences. These databases may require additional filtering because of higher redundancies. Curated databases, however, allow analysis focusing on biologically significant reference proteins with less redundancy. In the present study, reviewed sequence database from Uniprot/Swissprot was selected in order to perform reliable protein identification with evidence for relevant functions of proteins.

Subsequent to sequence searching, the significance of the acquired peptide identifications (IDs) is validated via various algorithms. Although top-scoring peptides are determined by search engines, the resulting PSMs may still be incorrect. Thus, the resulting peptide IDs need to be further evaluated. The most commonly used statistical values to validate putative IDs are *p*-value and false discovery rate (FDR).<sup>109</sup> By definition, *p*-value is the probability of obtaining a result equal to or more extreme than the actual observation, when assuming the *null hypothesis* is true. In the validation of PSMs, the null hypothesis can be that the peptide was not found by the MS analysis. Therefore, a low *p*-value indicates the possibility of the data occurring by chance is small when the null hypothesis is correct. For example, if one sets a threshold of *p*-value  $\leq 0.05$ , a 5% chance of false positives is allowed in a result. However, *p*-value threshold is usually considered as incomplete statistical validation value for large-scale samples. The 5% threshold in the example would cause a significant number of false

positives when one processes numerous tests. In order to overcome the multiple testing problem,  $p$ -value to each test may be adjusted or corrected based on the sample size. Among diverse approaches for correcting  $p$ -values, FDR is mainly used.<sup>110</sup> FDR is a ratio of false PSMs versus the total number of PSMs above a scoring threshold. Thus, FDR reduces the number of false positives by controlling the number of false discoveries from significant tests rather than all tests. In MS-based bioinformatics, a target-decoy method is often used to estimate FDR.<sup>111</sup> In this method, a decoy database is composed of reversed or shuffled sequences.<sup>111</sup> False peptide IDs are evenly distributed in both target and decoy databases, and then PSM FDR is determined as the number of decoy hits divided by the number of target hits.

Next, proteins IDs are inferred by grouping peptide IDs filtered at a given scoring criteria. For protein inference, ‘two-peptide rule’ is commonly applied, which requires a protein to contain two or more filtered peptides. More recently, ‘single-peptide rule’ has also received attention.<sup>112</sup> Proteins can be inferred by one or more peptides with this method, but peptide threshold is more stringent and lengths of peptides are also considered. Protein IDs are also evaluated by protein-level FDR estimation.

In addition to qualitative protein identification, quantification has become a fundamental topic in MS-based proteomics. MS was not originally designed for quantitative analysis because ESI efficiency and detectability of proteins or peptides are variable.<sup>113</sup> In recent decades, however, MS has emerged as a standard method for quantitative proteomics due to improvements in data processing methods.<sup>114</sup> Strategies for quantitative MS can be sorted into two major groups: labeling or label-free

quantitation. The most popular labeling method is stable-isotope labeling, which introduces signature mass tags to peptides or proteins by replacing specific atoms by their isotopes.<sup>114–118</sup> Labeling quantification can be either relative or absolute.

Label-free techniques attempt to quantify proteins or peptides without isotopic labeling.<sup>114</sup> Among various approaches of label-free quantification, spectral counting based on the number of PSMs has recently received substantial attention and is reported to result in a great dynamic range for quantitation and high reproducibility.<sup>119,120</sup> Spectrum counting is especially powerful for comparing large data sets, because the required information of spectral counts for each protein can be provided by search engines during protein identification.<sup>114</sup>

In this chapter, protein cargos of EVs from vegetative cells and sporulating cells were analyzed by bottom-up HPLC-MS/MS. The resulting spectra were processed by bioinformatics tools, and proteins from the two EV groups were quantitatively compared with a label-free spectral counting technique.

## **3.2 Materials and Methods**

### **3.2.1 Proteolysis**

EVs collected from all biological replicates at vegetative and sporulating phases were aliquoted for proteomic analysis. They were then lysed by 3 cycles of sonication for 40 sec on ice in 50 mM  $\text{NH}_4\text{HCO}_3$ , pH 7.8 with 8M urea and 1X protease inhibitor cocktail, (Sigma-Aldrich, St. Louis, MO). Each lysate was washed with 50 mM  $\text{NH}_4\text{HCO}_3$ , pH 7.8 through a 3kDa Amicon filter three times in order to dilute the urea



concentration down to 8 mM. Reduction of the lysates was performed with 20 mM DL-dithiothreitol for 30 min at 56°C, followed by alkylation with 40 mM iodoacetamide in the dark for 30 min at room temperature. Subsequently, the samples were digested by Sequencing Grade Trypsin Gold (Promega, Madison, WI) for 16 h at 37°C (enzyme to protein ratio: 1 to 30, w/w).

### **3.2.2 Peptide analysis by HPLC-MS/MS**

The tryptic peptides from the EVs were analyzed on a Shimadzu Prominence nano-HPLC (Shimadzu Scientific Instruments, Columbia, MD) interfaced with an LTQ-Orbitrap XL hybrid mass spectrometer (Thermo Fisher Scientific, San Jose, CA). Peptide mixtures from EVs containing 1 µg protein were injected onto an Acclaim PepMap 300 C18 trapping column (Dionex, Sunnyval, CA), stabilized and desalted by 95% solvent A (97.5% H<sub>2</sub>O, 2.5% acetonitrile, and 0.1% formic acid) with 5% solvent B (97.5% acetonitrile, 2.5% H<sub>2</sub>O, and 0.1% formic acid) for 10 min. Three technical replicates were injected from each of 3 biological replicates for EVs shed by vegetative and sporulating *B. subtilis* cells. The peptides were then separated on a reverse phase C18 analytical column (300 Å, 150 × 0.15 mm, Grace Davison Discovery Sciences, Columbia, MD) with a linear gradient increasing from 5% to 40% solvent B for 120 min, followed by a ramp from 40% to 85% for the next 25 min. The flow rate was set at 500 nL/min. Precursor ion scans were acquired in the Orbitrap with a resolution of 30,000 at m/z 400. The nine most abundant precursor ions were automatically chosen and fragmented by CID with a normalized collisional energy of 35 in each cycle. Product ions were scanned in the LTQ in a data-dependent mode. Three micro-scans

were averaged per a spectrum and a dynamic exclusion of 1 repeat count was enabled to exclude precursor ions previously scanned within 180 sec.

### 3.2.3 Bioinformatics

The resulting mass spectra were searched using the PepArML meta-search engine<sup>106</sup> in order to identify peptides and proteins. PepArML combined the results from seven search engines: Mascot, X!Tandem, KScore, MyriMatch, OMSSA, SScore, and InsPecT. A reference database of *B. subtilis* 168 proteins including 4,243 reviewed sequences was acquired from the UniProtKnowledgeBase (UniprotKB, July 2014). In the search parameters, trypsin was chosen for the proteolytic agent with carbamidomethylation of cysteine set as fixed modification and oxidation of methionine as variable modification. Maximal charge state was set as 4, and 1 missed cleavage was allowed. Additionally, precursor ion tolerance was  $\pm 2$  Da, while fragment ion tolerance was  $\pm 0.6$  Da. Flagella-associated proteins had non-overlapping identities and were removed. The search results from 3 technical replicates of each biological replicate were combined and filtered at 5% PSM FDR,<sup>111</sup> which was determined by PepArML. The proteins were required to contain two or more peptides, resulting in the final protein FDR  $\leq 0.25\%$ . Proteins identified from two or more peptides were then filtered at the FDR-corrected p-value  $\leq 0.05$  for multiple testing.<sup>120</sup> Subcellular locations, molecular functions, and biological processes of these proteins were annotated by the Protein Information Resource (PIR, [pir.georgetown.edu](http://pir.georgetown.edu)) based on Gene Ontology (GO) and UniprotKB. Database for Annotation, Visualization and Integrated Discovery (DAVID) bioinformatics resources<sup>121</sup> were also used for functional annotations.

The proteins identified with statistical significance were further analyzed for comparison of relative abundances between the vegetative EV proteome and the sporulating EV proteome. Spectral counting was processed based on the number of PSMs using an in-house software PepArML Spectral count 1.6.2. With this software, the difference in spectral counts of each protein between EVs from vegetative and sporulating cells was expressed as a ratio of spectral count,  $R_{sc}$ , according to the equation :  $R_{sc} = \log_2[(n_2+1.25)/(n_1+1.25)] + \log_2[(t_1-n_1+1.25)/(t_2-n_2+1.25)]$ , where  $n_1$  and  $n_2$  are the spectral counts of each protein from the two groups;  $t_1$  and  $t_2$  are the total numbers of spectra of the two groups; and 1.25 is a correction factor.<sup>120</sup> Differential p-values of spectral counts were also determined by the Fisher exact-test.

### **3.2.4 Western blot analysis**

Vegetative and sporulating *B. subtilis* cells and the two EV types were prepared as described in chapter 2 and lysed. Protein concentration of each lysate was determined by a BCA protein assay (Thermo Fisher Scientific, Rockford, IL). The four lysates were separated by one-dimensional SDS-PAGE. Each lysate containing 20  $\mu$ g total proteins were mixed with 2x Laemmli Sample Buffer (1:1, Bio-Rad, Hercules, CA) containing 5%  $\beta$ -mercaptoethanol, and the mixtures were incubated at 70°C for 15 min. The samples were then loaded on an 8–16% Criterion precast gel (Bio-Rad, Hercules, CA) and separated at 200 V for 40 min. Electrotransfer was performed for protein bands from the gel to a PVDF membrane (EMD Millipore, Billerica, MA) at 100 V for 1 h. The blots were blocked in 5% BSA and incubated with a primary antibody, a rabbit anti-*B. subtilis* alanine dehydrogenase polyclonal antibody at 1:35,000 dilution from a 2 mg/mL stock (LifeSpan BioSciences, Inc., Seattle, WA).

The primary antibody was tested with purified *B. subtilis* L-alanine dehydrogenase (Sigma-aldrich, St. Louis, MO). Secondary incubation was performed using an anti-rabbit IgG, horseradish peroxidase (HRP)-linked antibody at 1:2,000 dilution of a commercial stock solution (Cell signaling Technology, Beverly, MA). The blots were lastly incubated with SuperSignal West Dura extended duration substrate (Thermo Fisher Scientific, Waltham, MA) for detecting HRP. Image Lab System (Bio-Rad) with Gel-Doc program (Kodak Molecular Imaging Systems) was used for visualization of the blots. Relative intensities of the blots were estimated by Image J software.<sup>83</sup>

### **3.2.5 Alkaline phosphatase (AP) activity assay**

AP enzymatic activities in EVs were determined according to Lowry's colorimetric assay.<sup>122</sup> EVs containing 30 µg of proteins from each biological replicate were lysed as described above. The EV lysate was incubated with 100 µM *p*-nitrophenyl phosphate disodium salt hexahydrate (MP Bio, Santa Ana, CA) in AP assay buffer (1 M Tris-HCl, pH 7.8, 50 µM ZnCl<sub>2</sub>, 10 mM MgSO<sub>4</sub>) for 1 h at room temperature in the dark. The incubation was stopped with 0.5 M NaOH and UV absorbance at 405 nm of the samples was measured.

## **3.3 Results and discussion**

### **3.3.1 Characterization of EV proteins**

Proteins of EVs from vegetative and sporulating cells were analyzed by HPLC-MS/MS and searched using the PepArML meta search engine.<sup>106</sup> Three hundred and

forty nine proteins were identified based on two or more distinct peptides from vegetative EVs and 341 proteins from sporulating EVs with a final protein FDR of at most 0.25%. Out of a total of 417 unique proteins, 273 proteins were shared by the two groups. The identified proteins were additionally filtered with an FDR-corrected p-value  $\leq 0.05$ , resulting in 156 proteins from vegetative EVs and 185 proteins in sporulating EVs (Appendix 1). The two EV groups shared 133 proteins out of 208 proteins.

Subcellular locations and molecular functions of the filtered proteins were annotated with GO annotation using PIR (Figure 8, Figure 9). The subcellular locational distributions of the proteins were similar between vegetative EVs and sporulating EVs (Figure 9). The greatest number of proteins was sorted to membranes, followed by cytoplasm in both cases. A substantial difference in the ribosome category is due to more various and abundant ribosomal proteins in the sporulating EVs (Appendix 1). The annotations according to molecular functions of proteins were also similar in both groups (Figure 10). The total numbers of proteins identified with statistical significance and the numbers of unique peptides from the two populations of EVs were not substantially different in the proteomic results. In addition, more than 70% of total proteins identified from each group was present in both EV populations. Quantitative comparisons were more revealing.

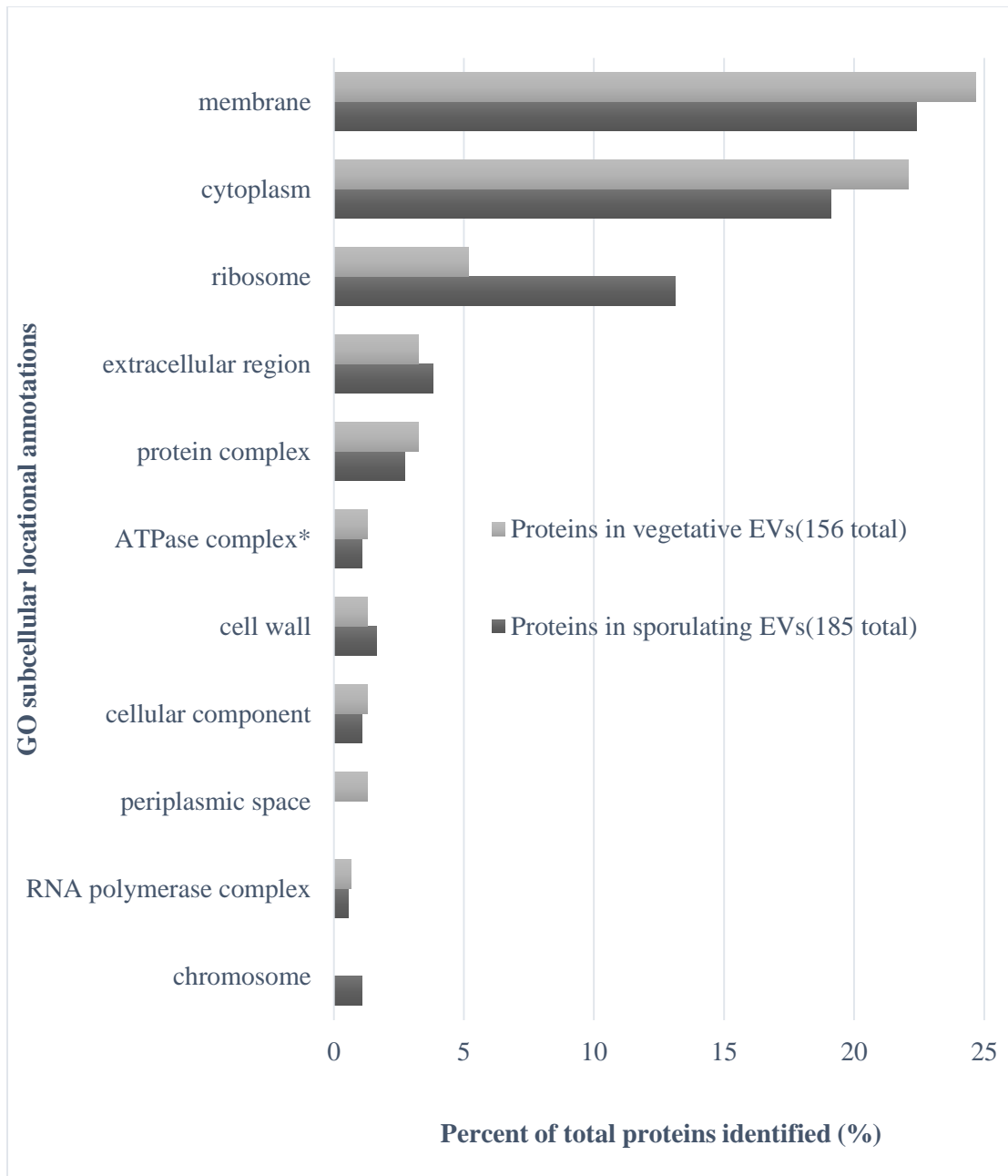


**Figure 9.** Subcellular locational distributions of identified proteins based on Gene Ontology (FDR-corrected p-values  $\leq 0.05$ ). The most highly assigned 10 locations from each EV group were selected (annotation p-value  $\leq 0.05$ ). Some proteins were located to more than one category. Unclassified proteins were not included. \*proton-transporting two-sector ATPase complex.

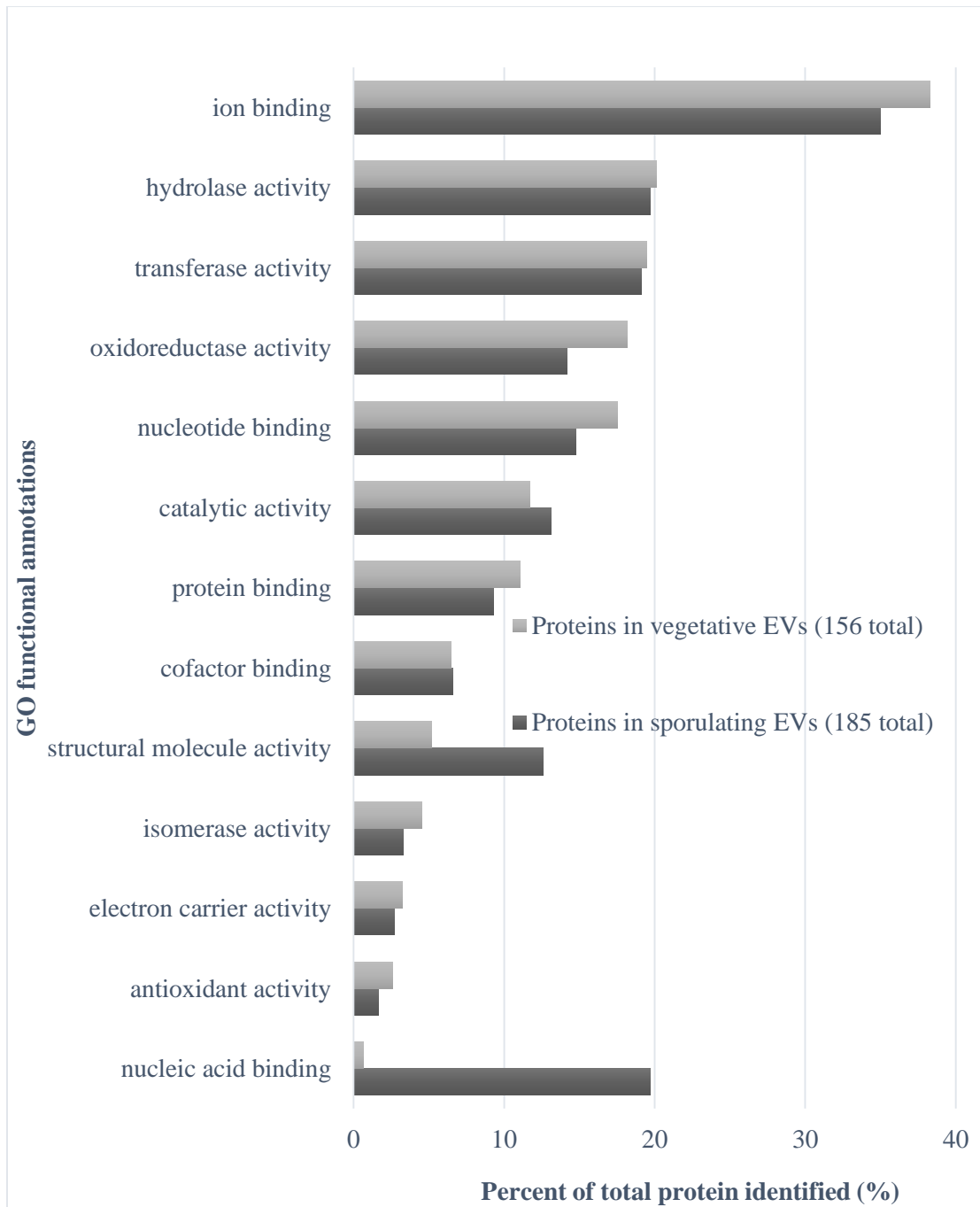


**Figure 10.** Molecular functional annotations of identified proteins based on Gene Ontology (FDR-corrected  $p$ -value  $\leq 0.05$ ). The most highly populated 10 functions from each EV group were selected (annotation  $p$ -value  $\leq 0.05$ ). Some proteins were located to more than one category. Unclassified proteins were not included.

### 3.3.2 Relative abundances of proteins

Relative abundances of identified proteins were determined by spectral counting and expressed as  $R_{sc}$ , which is the  $\log_2$  ratio of spectral counts for each protein in vegetative EVs versus sporulating EVs or that in sporulating EVs versus vegetative EVs. Proteins with  $R_{sc} > 1$  in each case were considered to have substantially higher abundances (>2-fold) in a group.  $R_{sc}$  was calculated for the 208 total distinct proteins. Seventy-five proteins out of 208 had significantly greater abundance in vegetative EVs than sporulating EVs, while 124 proteins had greater abundance in sporulating EVs with a high reliability (Table 1, 2, and Appendix 1). However, it is noteworthy that 70% of the cells in sporulating culture contained endospores.

GO biological processes for the proteins with differential abundances were assigned using PIR (Figure 11). Proteins more abundant in vegetative EVs were mostly involved in metabolic processes. Also, a substantial number of proteins in vegetative EVs were annotated to participate in processes of response to stimulus. For the proteins more abundant in sporulating EVs, however, metabolic functions were significantly decreased. Instead, proteins involved in processes critical for cellular differentiation such as ribosome biogenesis, sporulation, locomotion, and cell division were enriched. The number of proteins for response to stimulus remained similar to that of vegetative EVs. Functional pathways according to KEGG for proteins with different abundances were clustered using DAVID.<sup>121</sup> Five functional pathways from each group were annotated with a reliable annotation p-value (<0.05) (Table 3). The pathways associated with metabolism were mostly enriched in vegetative EV proteins, while pathways for ribosome biogenesis and chemotaxis were additionally enriched in



sporulating EV proteins. Therefore, the relative abundances of individual proteins differed significantly between the two EV groups. The proteins with differential abundances were observed to be involved in different biological processes. These results indicate that *B.subtilis* EVs carry different protein components depending on the developmental phases of parental cells.

**Table 1.** List of proteins with greatest 50  $R_{SC}$  from vegetative EVs (FDR-corrected p-value  $\leq 0.05$ )

<b>Proteins significantly more abundant in vegetative EVs</b>		
<b>Uniprot Accession</b>	<b>Description</b>	<b><math>R_{SC}^a</math></b>
P80860	Glucose-6-phosphate isomerase	6.8
P37253	Ketol-acid reductoisomerase	6.2
Q04789	Acetolactate synthase	6.0
O34348	Fe(3+)-citrate-binding protein YfmC	5.9
P37942	Lipoamide acyltransferase component of branched-chain alpha-keto acid dehydrogenase complex	5.7
P42199	L-cystine-binding protein TcyA	5.4
P94521	Putative aminopeptidase YsdC	5.3
O34924	Putative aminopeptidase YtoP	5.1
P24327	Foldase protein PrsA	4.9
P39751	MreB-like protein	4.4
P80700	Elongation factor Ts	4.3
P21881	Pyruvate dehydrogenase E1 component subunit alpha	4.2
P19582	Homoserine dehydrogenase	4.2
P80239	Alkyl hydroperoxide reductase subunit C	4.2
P11998	6,7-dimethyl-8-ribityllumazine synthase	4.2
O07603	Putative aminopeptidase YhfE	4.1

<b>Uniprot Accession</b>	<b>Description</b>	<b>R<sub>sc</sub><sup>a</sup></b>
O34866	Putative carboxypeptidase YodJ	4.0
P26900	L-asparaginase 1	3.9
P49814	Malate dehydrogenase	3.8
P80879	General stress protein 20U	3.7
P20429	DNA-directed RNA polymerase subunit alpha	3.64
P40924	Phosphoglycerate kinase	3.63
P45694	Transketolase	3.57
O34860	RsbT co-antagonist protein RsbRB	3.54
P28598	60 kDa chaperonin	3.45
O32106	Probable cytosol aminopeptidase	3.43
P05653	DNA gyrase subunit A	3.39
P42974	NADH dehydrogenase	3.36
P29727	GMP synthase [glutamine-hydrolyzing]	3.25
P37870	DNA-directed RNA polymerase subunit beta	3.21
P46911	Menaquinol-cytochrome c reductase iron-sulfur subunit	3.18
Q02112	Membrane-bound protein LytA	3.18
P39773	2,3-bisphosphoglycerate-independent phosphoglycerate mutase	3.11
P55910	L-lactate permease	2.96
P26901	Vegetative catalase	2.94
P09124	Glyceraldehyde-3-phosphate dehydrogenase 1	2.90
C0SP94	Putative ABC transporter substrate-binding lipoprotein YhfQ	2.89
P08495	Aspartokinase 2	2.80
P42409	RsbT co-antagonist protein RsbRA	2.70
P37941	2-oxoisovalerate dehydrogenase subunit beta	2.69
P94356	Uncharacterized protein YxkC	2.65
P54616	Enoyl-[acyl-carrier-protein] reductase [NADH] FabI	2.61
P96499	Putative transcriptional regulator YvhJ	2.58

Uniprot Accession	Description	R <sub>SC</sub> <sup>a</sup>
P21882	Pyruvate dehydrogenase E1 component subunit beta	2.54
P22326	Tyrosine--tRNA ligase 1	2.50
P54326	Phage-like element PBSX protein XkdF	2.47
P13243	Probable fructose-bisphosphate aldolase	2.46
P39594	Thiamine-phosphate synthase	2.43
O34752	Prolipoprotein diacylglyceryl transferase	2.39
P54547	Glucose-6-phosphate 1-dehydrogenase	2.39

$$^a R_{SC} = \log_2 \left( \frac{n_{vegetative} + 1.25}{n_{sporulating} + 1.25} \right) + \log_2 \left( \frac{f_{sporulating} - n_{sporulating} + 1.25}{f_{vegetative} - n_{vegetative} + 1.25} \right)$$

**Table 2.** List of proteins with greatest 50 R<sub>SC</sub> from sporulating EVs (FDR-corrected p-value ≤ 0.05)

Proteins significantly more abundant in sporulating EVs		
Uniprot Accession	Description	R <sub>SC</sub> <sup>b</sup>
P21466	30S ribosomal protein S4	8.5
P21469	30S ribosomal protein S7	8.1
P42919	50S ribosomal protein L2	7.6
P26908	50S ribosomal protein L21	7.4
P21473	30S ribosomal protein S15	7.3
P19405	Alkaline phosphatase 3	7.0
O31742	50S ribosomal protein L19	6.9
O34469	Putative ATP-dependent helicase YeeB	6.9
P46899	50S ribosomal protein L18	6.4
P12877	50S ribosomal protein L5	6.3
P19946	50S ribosomal protein L15	6.1
P40406	Beta-hexosaminidase	5.8
P54325	Phage-like element PBSX protein XkdE	5.6

<b>Uniprot Accession</b>	<b>Description</b>	<b>R<sub>sc</sub><sup>b</sup></b>
P42060	50S ribosomal protein L22	5.6
O31550	Dihydrolipoyllysine-residue acetyltransferase component of acetoin cleaving system	5.4
P04969	30S ribosomal protein S11	5.4
Q45598	Uncharacterized protein YydD	5.4
O34450	N-acetylglucosamine-6-phosphate deacetylase	5.4
P54507	Spore coat-associated protein N	5.3
P54332	Phage-like element PBSX protein XkdM	5.3
P28628	Signal peptidase I S	5.24
P05657	50S ribosomal protein L27	5.18
P21475	30S ribosomal protein S18	5.18
P46898	50S ribosomal protein L6	5.14
O32258	Uncharacterized glycosylase YvbX	5.03
Q06796	50S ribosomal protein L11	4.92
Q45596	Putative exported peptide YydF	4.92
P20166	PTS system glucose-specific EIICBA component	4.91
O34662	Uncharacterized aminotransferase YodT	4.85
P21467	30S ribosomal protein S5	4.85
P94421	Uncharacterized ABC transporter solute-binding protein YclQ	4.85
P54339	Phage-like element PBSX protein XkdT	4.83
O31740	Ribosome maturation factor RimM	4.69
P24137	Oligopeptide transport ATP-binding protein OppF	4.61
P71021	Septum site-determining protein DivIVA	4.40
P21464	30S ribosomal protein S2	4.23
P45921	Uncharacterized protein YqbE	4.21
P39456	L-cystine import ATP-binding protein TcyC	4.20
P54560	DNA polymerase IV 2	4.20
P55873	50S ribosomal protein L20	4.20

<b>Uniprot Accession</b>	<b>Description</b>	<b>R<sub>SC</sub><sup>b</sup></b>
P0CI73	Glutamine--fructose-6-phosphate aminotransferase [isomerizing]	4.15
P17904	Serine-protein kinase RsbW	4.08
P30949	Glutamate-1-semialdehyde 2,1-aminomutase	3.94
P54340	Phage-like element PBSX protein XkdU	3.94
P54327	Phage-like element PBSX protein XkdG	3.93
O31927	SPBc2 prophage-derived uncharacterized protein YopK	3.79
O32072	Uncharacterized protein YtwF	3.79
P37471	Cell division protein DivIC	3.79
P71012	PTS system fructose-specific EIIABC component	3.76
Q45597	Fructose-1,6-bisphosphatase class 3	3.76

$${}^b R_{SC} = \log_2 \left( \frac{n_{sporulating} + 1.25}{n_{vegetative} + 1.25} \right) + \log_2 \left( \frac{f_{vegetative} - n_{vegetative} + 1.25}{f_{sporulating} - n_{sporulating} + 1.25} \right)$$

**Table 3.** Enriched KEGG (Kyoto Encyclopedia of Genes and Genomes) pathways annotated in the two EV samples (p-values evaluate annotations)

<b>KEGG pathways of vegetative EVs</b>	<b>Count</b>	<b>Fisher's p-value</b>	<b>KEGG pathways of sporulating EVs</b>	<b>Count</b>	<b>Fisher's p-value</b>
Glycolysis / Gluconeogenesis	10	6.5E-06	Ribosome	22	1.6E-12
Citrate cycle (TCA cycle)	5	0.0015	Sphingolipid metabolism	2	0.0016
Pyruvate metabolism	6	0.0053	RNA degradation	3	0.0082
Valine, leucine and isoleucine biosynthesis	5	0.012	Fatty acid biosynthesis	3	0.013
Pentose phosphate pathway	5	0.0044	Bacterial chemotaxis	4	0.016

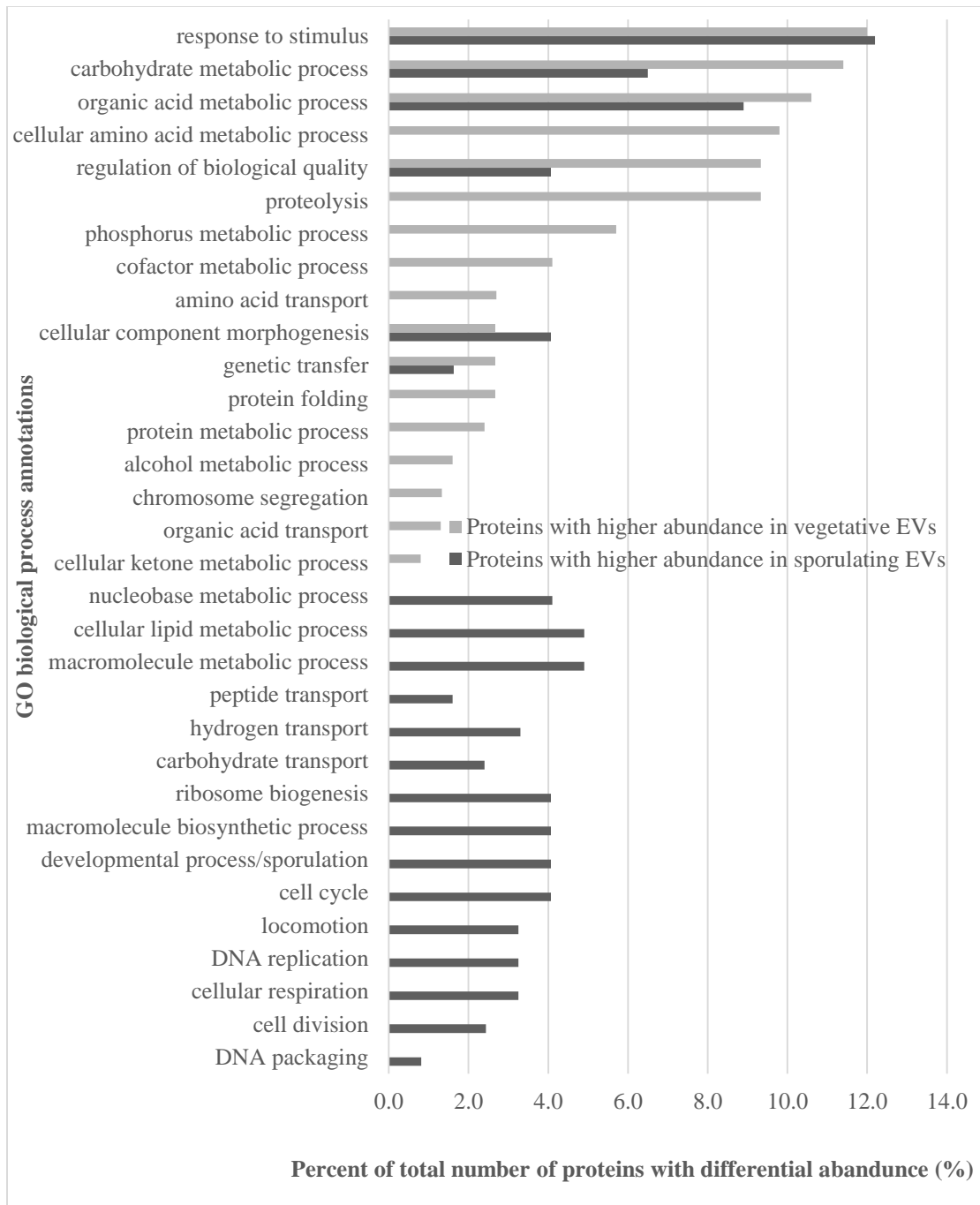


**Figure 11.** Biological process annotations of proteins with  $R_{SC} > 1$  based on Gene Ontology. Biological processes of 75 proteins more abundant in vegetative EVs and 124 proteins more abundant in sporulating EVs were annotated (annotation p-values  $\leq 0.05$ ). Unclassified proteins were not included.

### 3.3.3 Sporulation-associated proteins

Proteins known to participate in bacterial sporulation were found from the 208 total proteins. Nine sporulation-associated proteins were highly enriched or only found in sporulating EVs (Table 4).

**Table 4.** List of sporulation-associated proteins identified from sporulating EVs

Accession	Sporulation-associated proteins	R <sub>sc</sub> <sup>a</sup>	FDR-p-value	GO-BP annotation
P19405	Alkaline phosphatase III	7.0	2.34E-63	metabolic process
P54507	Spore coat-associated protein N <sup>b</sup>	5.3	4.37E-11	Sporulation
P24137	Oligopeptide transport ATP-binding protein OppF (Stage 0 sporulation protein KE)	4.6	1.76E-11	Sporulation
P71021	Septum site-determining protein DivIVA	4.4	1.46E-36	Sporulation
P37471	Cell division protein DivIC <sup>b</sup>	3.8	0.00032	cell cycle
P24136	Oligopeptide transport ATP-binding protein OppD (Stage 0 sporulation protein KD)	3.8	2.97E-06	Sporulation
O31529	Beta-galactosidase YesZ	3.3	5.56E-06	metabolic process
P39623	Spore coat polysaccharide biosynthesis protein SpsC <sup>b</sup>	2.7	0.037	metabolic process
Q08352	Alanine dehydrogenase (Stage V sporulation protein N)	1.3	9.14E-05	Sporulation

<sup>a</sup> R<sub>sc</sub> of sporulating EV proteins over vegetative EV proteins. The proteins with R<sub>sc</sub> >1 were considered to be significantly more abundant in sporulating EVs.

<sup>b</sup> Proteins identified only from sporulating EVs.

\*GO-BP annotation: Gene Ontology biological process annotation

Five out of the 9 proteins, named spore coat associated protein N (tasA), oligopeptide transport ATP-binding protein OppD (alternative name: stage 0 sporulation protein KD Spo0KD), oligopeptide transport ATP-binding protein OppF (stage 0 sporulation protein KE Spo0KE), septum site-determining protein DivIVA and alanine dehydrogenase (alternative name : stage V sporulation protein N spoVN) were clustered into sporulation according to GO annotation (Figure 11, Table 4). Concretely, tas A has been proposed to be secreted into the extracellular region during early sporulation and have a broad spectrum of antibiotic activities against other bacteria.<sup>123</sup> The observation of tas A in EVs suggests that shedding of EVs is a secretion pathway of tasA. Oligopeptide permeases OppD (Spo0KD) and OppF (Spo0KE) are parts of the oligopeptide transport system, which is a well-known recycling pathway in Gram-negative bacteria.<sup>124</sup> Furthermore, these proteins have been reported to play an important role in the initiation of sporulation.<sup>124-127</sup> OppF has less impact than OppD, while OppD is indispensable for sporulation.<sup>126</sup> General function of DivIVA is to control the cell division sites in either vegetative or sporulating *B.subtilis*.<sup>128</sup> DivIVA has been observed to be critical for polar localization of the chromosome, which results in formation of an asymmetric septum during sporulation.<sup>128-130</sup> Alanine dehydrogenase (spoVN) catalyzes oxidative deamination of L-alanine to pyruvate. This enzyme has been shown to function in absorption of L-alanine during sporulation.<sup>131</sup> The presence and the relative abundance of spoVN between vegetative and sporulating EV types were confirmed by western blotting with anti-*B. subtilis* spoVN antibody. SpoVN blot in sporulating EV lysate showed a stronger band intensity for spoVN than that in vegetative EV lysate by about 2.4-fold. This observation is consistent to the



spectral counting result quantitatively (Figure 12, Table 4). Sporulating cell lysate also showed a higher spoVN band intensity relative to vegetative cell lysate, suggesting abundance of this protein in EVs reflects the developmental phases of *B. subtilis* cells (Figure S4). Identifications of these proteins annotated for sporulation were manually confirmed in mass spectra (Figure 13).

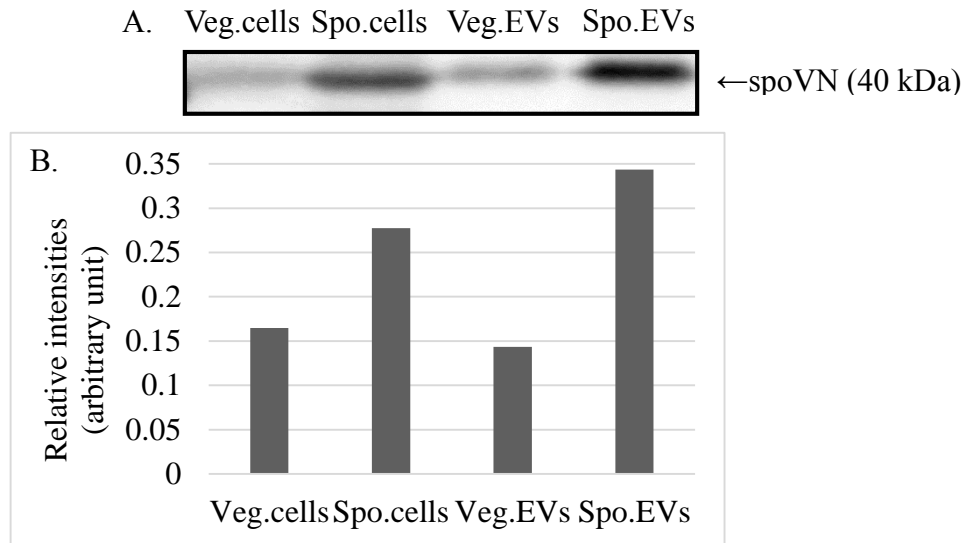


**Figure 12.** Western blotting of alanine dehydrogenase (stage V sporulation protein N, spoVN) in lysates of cells and EVs. (A) Western blot (8-16% SDS-PAGE) of spoVN in vegetative cell lysate (Veg.cells), sporulating cell lysate (Spo.cells), lysate of EVs from vegetative cells (Veg.EVs), and lysate of EVs from sporulating cells (Spo.EVs) with anti-spoVN polyclonal antibody. (B) Relative band intensities of spoVN blots. Intensities were determined relative to a band of positive control (purified *B. subtilis* alanine dehydrogenase) using Image J.

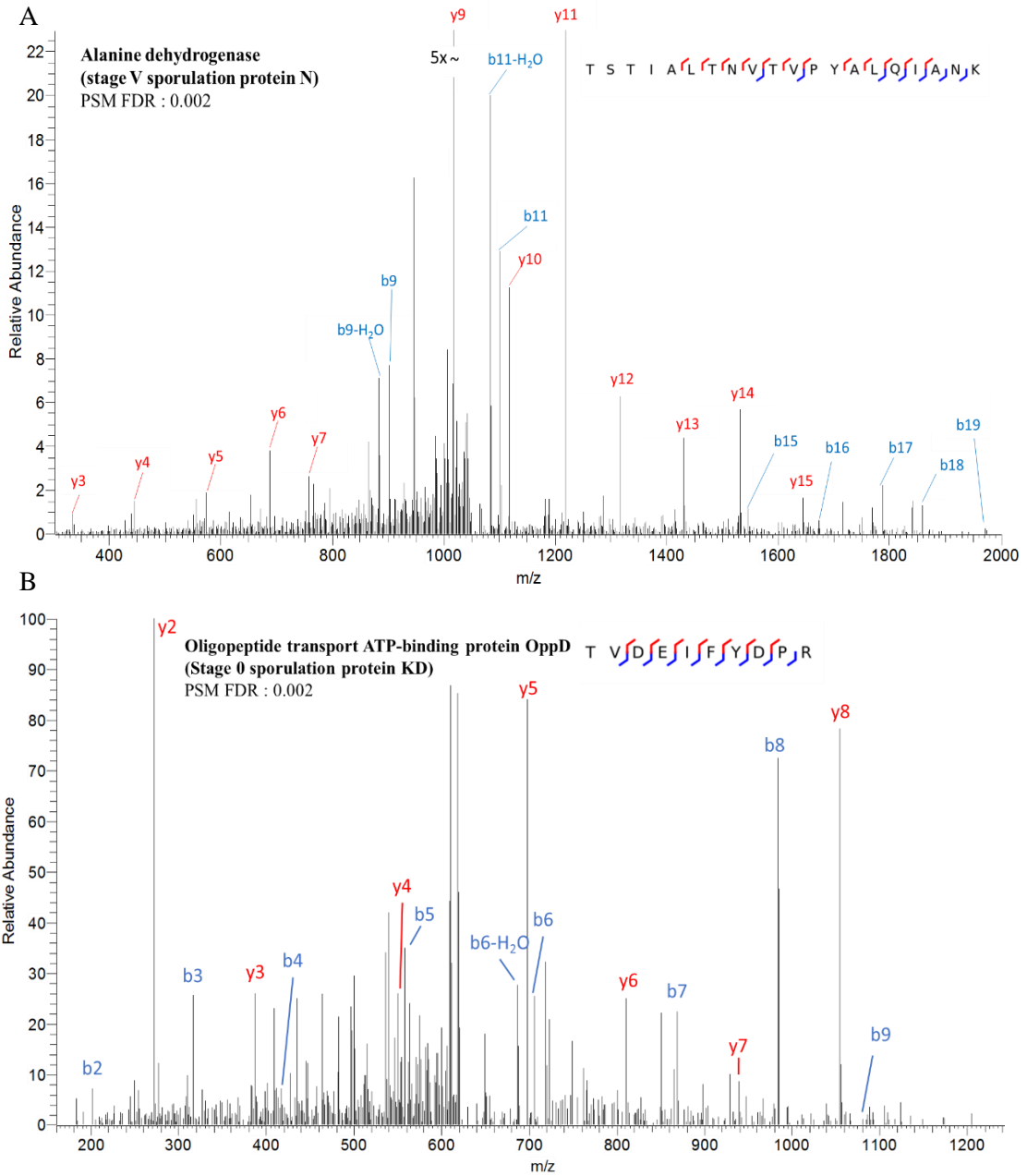


**Figure 13.** MS/MS spectra of sporulation-associated proteins. (A) a peptide from alanine dehydrogenase. (B) a peptide from oligopeptide transport ATP-binding protein OppD.

In addition, sporulation stage-specific marker proteins were also identified with greater abundance in sporulating EVs. AP and  $\beta$ -galactosidase are considered as a sporulation stage II specific marker protein and a stage III marker protein, respectively.<sup>55,56,132,133</sup> Enzymatic activities of AP and  $\beta$ -galactosidase have been widely used to screen the progress of sporulation.<sup>55,134</sup> AP enzymatic activity assays for the EVs showed a qualitatively consistent result with the spectral counting (Figure 14).

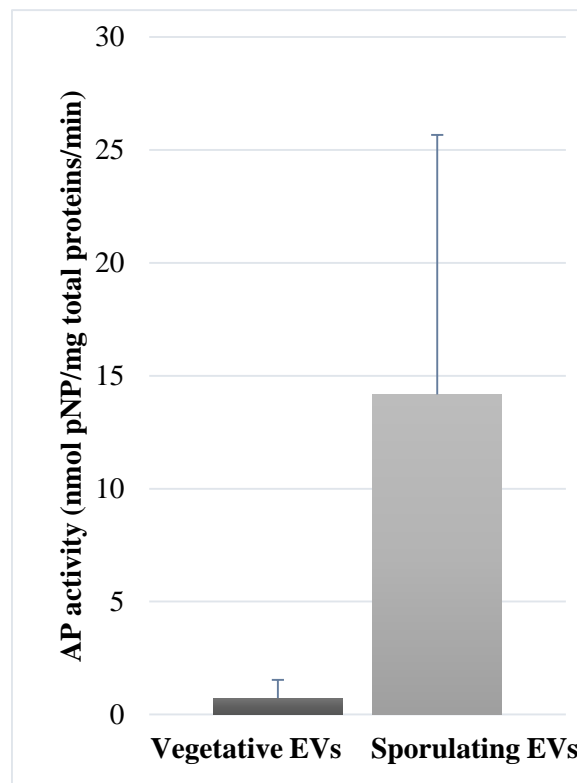


**Figure 14.** Alkaline phosphatase activities from EV protein cargos (n=3). pNP: *p*-nitrophenol

Explainfully, AP enzymatic activities in sporulating EVs were substantially higher than those in vegetative EVs from all three biological replicates. AP III was the

only type of AP identified in this study, and it has been reported to have the greatest correlation with sporulation among the *B.subtilis* AP family.<sup>135</sup> Unlike other APs, the production of AP III is independent of phosphate starvation and rapidly increases during sporulation.<sup>135</sup> Cell division protein DivIC and spore coat polysaccharide biosynthesis protein SpsC were also reviewed to participate in sporulation according to previous publications,<sup>136,137</sup> although they were not annotated for sporulation by GO annotation. DivIC has been shown to participate in the activation of gene expression controlled by transcription factors for sporulation, as well as in the cellular septum formation.<sup>136</sup> SpsC has been proposed to be essential for spore-surface polysaccharides synthesis but it may need to be further studied.<sup>137</sup>

Besides sporulation-specific proteins, the protein groups of phage-like element PBSX proteins, ribosomal proteins, and methyl-accepting chemotaxis proteins were also highly enriched in sporulating EVs (Table 2, Appendix 1). These proteins have not shown direct correlation with the sporulation process, but they may be indirectly related to it. First, the phage-like element PBSX proteins have been found to respond to stimulants such as SOS- or sporulation-inducing signals, resulting in the release of phage-like particles, which may kill other bacteria.<sup>138</sup> Second, ribosomal proteins were also more abundant and diverse in sporulating EVs than vegetative EVs. In addition to structuring ribosome, ribosomal proteins may function in other diverse processes such as improving antibiotic resistance, integrating translation with other cellular pathways, and responding to stress.<sup>139</sup> EVs may carry the ribosomal proteins to support the spore formation or to respond to environmental stressors. Another unexpected protein group was methyl-accepting chemotaxis proteins (Appendix 1), which are known to mediate

mobility, responding to numerous attractants or repellents.<sup>140</sup> They may be suggested to participate in sporulation by responding to nutrient depletion.

### **3.4 Summary**

In the results of protein identifications obtained by proteomic methods, the total numbers of EV proteins identified and the numbers of unique peptides were comparable between vegetative EVs and sporulating EVs with more than 70% shared proteins. The distributions for the subcellular locations and the molecular functions of proteins were also similar between them. In the comparison of spectral counts, however, the relative abundance of each protein changed markedly, indicating the components in EVs are affected by growth stages of parental cells. This observation supports the general hypothesis that the shedding of EVs from cells is for distinct biological purposes. In particular, the EVs from sporulating cells contained significantly more proteins contributing directly and indirectly to spore formation. These proteins suggest that EVs may be a novel means for intercellular communication delivering sporulation-inducing proteins. In addition, proteins present, which respond to stresses and have antibiotic activity, were found in both EV types with higher abundances in sporulating EVs. These proteins showed possible functions of EVs in bacterial viability.

## **Chapter 4: Observation of interaction between *B. subtilis***

### **cells and EVs**

#### **4.1 Introduction**

As a number of biologically functional components are carried by EVs from diverse organisms, it is proposed that EVs may participate in intercellular communications and host-pathogen interactions. Previous studies for internalizations of EVs or EV components into either eukaryotic or prokaryotic cells have supported this hypothesis.<sup>1,2,141,142</sup> Endocytosis and membrane fusion are the two main pathways for internalization.<sup>76</sup> The trafficking mechanism of EV components into bacterial cells is considered to be carried out by membrane fusion rather than endocytotic uptake, which is expected to occur only in eukaryotes. Although endocytosis-like uptake of proteins to bacterial cells has been reported, it is limited to the small number of bacterial species that show subcellular compartmentalization.<sup>143</sup> The interaction of EVs from Gram-negative bacteria with both Gram-negative and -positive bacterial cells has been observed.<sup>15</sup> However, the communication between Gram-positive bacterial EVs and their parental cells has not been studied.

We and others have found that Gram-positive bacteria naturally shed EVs. In the previous chapter, *B. subtilis* EVs were shown to carry quantitatively different proteins, which have biological functions reflecting the two growth phases. This suggests that EV proteins have active functions in bacterial life. With these evidence

and assumption, an important unanswered question is how the contents in EVs can be delivered into bacterial cells in a population.

High-resolution microscopy and the use of fluorescence probes have emerged as powerful techniques to examine cell-to-cell, particle-to-cell, or particle-to-particle interactions. For example, TEM with thin-sectioning and gold particle labeling techniques have shown that the membrane fusion of EVs occurs at bacterial cell membranes and that the bacterial cells lyse because of the fusion.<sup>15</sup>

Confocal microscopy is the most widely used method among various fluorescence microscopic techniques. In the study of EVs, relatively long-chains of lipophilic fluorescence dyes are often incorporated to overcome the limit of resolution for nano-scaled sizes. Using this technique, endocytotic uptake of EVs to eukaryotic cells and, rarely, membrane fusion have been observed.<sup>141,142,144</sup> Deconvolution microscopy is considered to be a powerful alternative of confocal microscopy using computational algorithms, which remove blur of images.<sup>145,146</sup> In general, this image processing is applied for wide-field microscope, but more recently, confocal micrographs have also been analyzed by deconvolution algorithms.<sup>145</sup> Modern deconvolution techniques have showed resolution comparable to that from confocal microscopy. Deconvolution microscopy may be better for dim images of relatively small objects.

In addition, assays optimized for membrane fusion using fluorescence probes are available such as NBD–rodamine energy transfer<sup>147</sup> and octadecyl rhodamine B self-quenching.<sup>148</sup> These methods allow successive and relatively accurate measurement of membrane fusion. Using the fluorescence-based fusion approaches,

changes of fusion efficiency can also be estimated for EVs at varied environmental conditions.<sup>149</sup> In this chapter, fluorescence microscopy with a deconvolution technique and fluorescence spectrophotometry were used to characterize the interaction between *B. subtilis* cells and their EVs.

## **4.2 Materials and Methods**

### **4.2.1 Deconvolution fluorescence microscopy**

An aliquot of the sporulating EVs containing 100 µg of proteins was incubated with 5 µM DiD lipophilic dye for 15 min. Excess dye was removed by ultracentrifugation at 200,000 ×g for 90 min in 25 mL PBS. The pellet of DiD-bound EVs was resuspended in PBS. One colony of *B. subtilis* cells grown on BHI-agar plate was washed in PBS by centrifugation at 10,000 ×g for 3 min and suspended in PBS. The cells were incubated with the stained EVs for 0, 2, 5, 10, 20, 40, and 60 min. At each time point, 1/7 of the total volume was aliquoted and washed in PBS by centrifugation at 10,000 ×g for 3 min. The time point at 0 min indicates cells before the addition of stained EVs. The resulting pellets of incubated cells were then fixed in 4% paraformaldehyde for 10 min at room temperature and 50 min on ice.<sup>150</sup> Lastly, the incubated cells were washed with PBS five times and mounted on slides with a final concentration of 1.5% low melting point agarose containing 0.5 µg/mL DAPI. All centrifugation steps were processed at 4 °C. For dead cell-EV interaction test, the *B. subtilis* cells were pre-fixed with paraformaldehyde before the incubation with EVs. Images were acquired and developed using a 60X oil-immersion objective on an



Olympus IX-71 inverted microscope linked to a DeltaVision deconvolution imaging system (Applied Precision, Issaquah, WA). Excitation filters of 390/18 and 632/22, and emission filters of 435/48 and 679/34 are used for DAPI and DiD, respectively. The fluorescence intensities of the cell membranes were determined using Image J software.<sup>83</sup>

#### **4.2.2 Membrane fusion assay**

The possibility of fusion between EVs and *B. subtilis* cells was tested using octadecyl rhodamine B chloride (R18, Hayward, CA), a self-quenching lipophilic dye.<sup>148,151</sup> EVs isolated from sporulating *B. subtilis* cells, containing 25 µg of proteins were labeled with 30 µM ethanolic R18 probes in a staining buffer (50 mM Na<sub>2</sub>CO<sub>3</sub> and 130 mM NaCl, pH 8.5)<sup>144</sup> at room temperature for 1 h. The R18-labeled EVs were washed with 200 mM NaCl in PBS twice by ultracentrifugation at 150,000 ×g for 70 min. The final pellet of EVs was resuspended in the washing buffer. A single colony of *B. subtilis* cells grown in BHI agar were prepared by washing in PBS and pelleted at 10,000 ×g for 3 min. They were then resuspended in the washing buffer. The fluorescence of R18 labeled to EVs was measured continuously using the F-4500 fluorescence spectrophotometer for 35 min with excitation at 560 nm and emission at 590 nm with slits of 2.5 nm. The time scans were produced at room temperature with gentle shaking. After suspension of the EV for 5 min as an equilibration step, one-fifth of the prepared cells were added. The incubation was stopped by adding Triton X-100 at a final concentration of 0.3%, resulting in the maximum of R18 fluorescence. The fluorescence of R18-labeled EVs at each second was expressed as percent of maximal

fluorescence de-quenching (FD) according to an equation  $\%FD = [(F-F_i)/(F_{max}-F_i)] \times 100$ , where  $F$  indicates the fluorescence intensity at each time point,  $F_i$  is initial fluorescence of R18-labeled EVs before the injection of cells, and  $F_{max}$  represents the maximal intensity after the injection of Triton X-100.

### 4.3 Results and discussion

All possible interaction pathways between EV and bacterium should be considered. Fluorescence microscopy was initially chosen to examine the unknown interactions. Specifically, a long-chain lipophilic dye and wide-field fluorescence microscope with Deltavision deconvolution software were used to visualize nano-scaled EVs. In the test of dyes, DiD-labeled and DiO-labeled EVs were successfully detected on a Deltavision deconvolution microscope (Figure 15).

Subsequently, DiD-stained EVs were incubated with live and dead (pre-fixed) *B. subtilis* cells separately (Figure 16). Internalization of intact EVs by endocytosis-

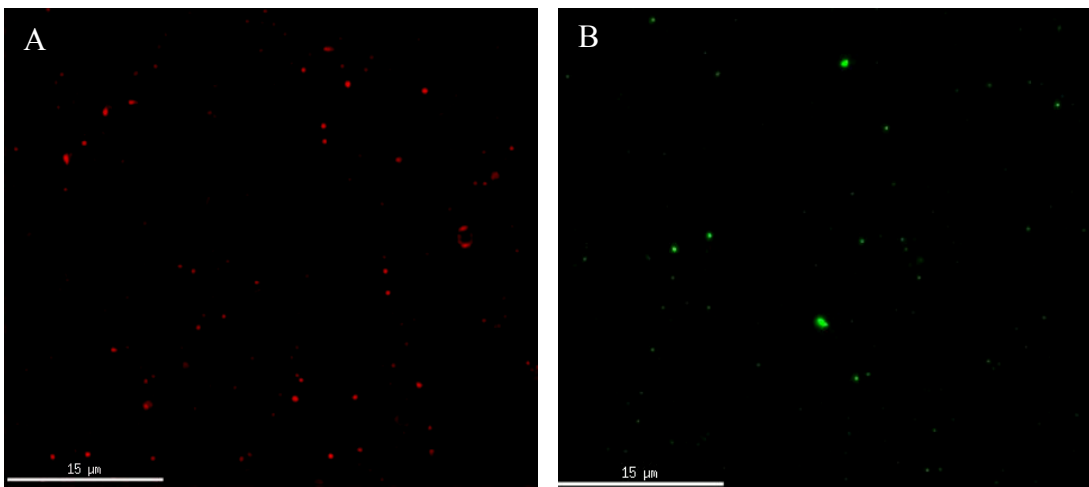


**Figure 15.** Deconvolution fluorescence microscopic images of EVs. *B. subtilis* EVs stained with (A) DiD and (B) DiO lipophilic dyes.

like uptake may result in intense DiD fluorescence as clear dots inside the cells, while membrane fusion would show diluted signals spread over the cell membrane.

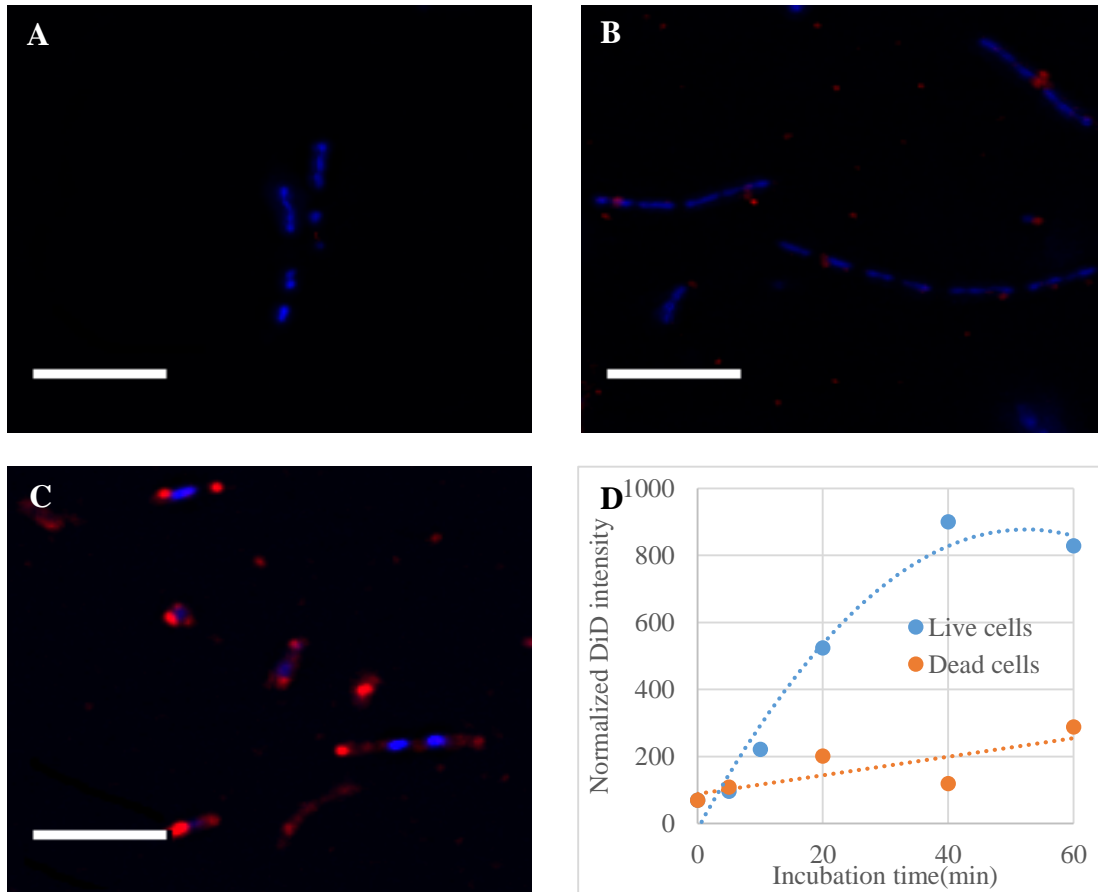


**Figure 16.** Deconvolution fluorescence images. (A) DAPI-stained *B. subtilis* cells (0 min incubation), (B-C) Cells incubated with DiD labeled EVs for (B) 3 min, (C) 60 min (representative images from 100-200 cells per time). DAPI labeled to chromosomes is in blue and DiD initially labeled to EVs is in red. (D) Normalized DiD fluorescence intensity on cell membranes over incubation time (Each single dot represents an average of >30 cell membranes). Intensities were measured with Image J. Scale bars: 5  $\mu$ m

Endocytotic uptake was not seen. Instead, the red fluorescence signal on cell membrane was slightly enhanced as incubation time increased, suggesting fusion of the EVs into cell membrane (Figure 16). Also, the increase of red fluorescence intensity is higher in live cell incubation relative to dead cell incubation (Figure 16D). However, the overall increase of red fluorescence intensity was not strong and variability was broad across multiple cells. If fusion is occurring between cells and EVs, these results could be due to the fast dynamics of the fusion events and substantial dilution of DiD dye.<sup>2</sup> Therefore, their interaction may be difficult to be visualized and quantified by fluorescence microscopy.

Next, the fusion event between EVs and the cells was tested using fluorescence de-quenching measurement of the lipophilic probe R18. The R18 dyes are expected to be de-quenched by dilution of the probes resulting from lipid mixing. Their fluorescence would subsequently increase. The EVs were labeled with R18 and unlabeled *B. subtilis* cells were added after 5 min. The injection of *B. subtilis* cells induced a strong increase of the R18 fluorescence, suggesting that membrane fusion-like events occurred between EVs and cells (Figure 17).

As discussed previously, EVs would have difficulty contacting the Gram-positive bacterial cell membrane because of the peptidoglycan layer on outmost cell surface. In the proteomic results from the previous chapter, cell wall hydrolytic enzymes were identified in EVs from both vegetative and sporulating cells (peptidoglycan DL-endopeptidase CwlO and N-acetylmuramoyl-L-alanine amidase LytC) (Appendix 1). These autolysins in EVs may disrupt the peptidoglycan layer on *B. subtilis* cells and promote the contact between EVs and cell membranes.

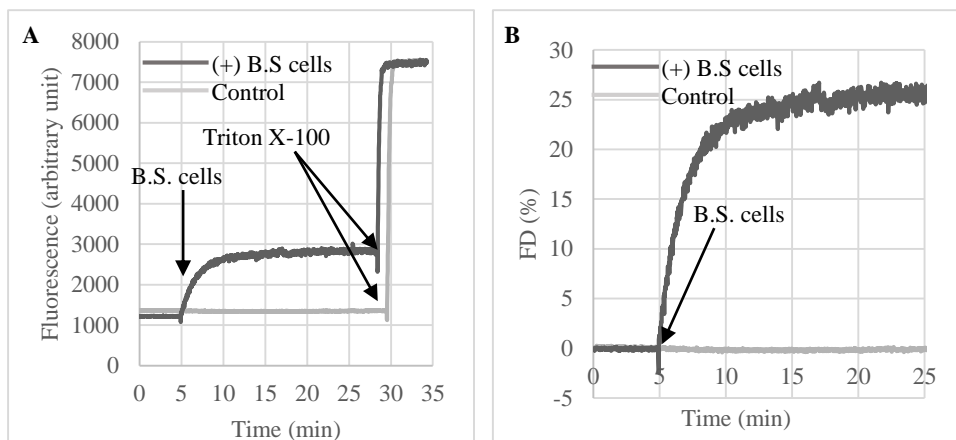


**Figure 17.** Fluorescence spectrophotometric detection of membrane fusion-like interaction between EVs and *B. subtilis* cells. (A) Fluorescence intensities of R18-labeled EVs (sporulating) following addition of cells, and subsequent disruption with Triton X100. (B) The percent of fluorescence de-quenching (FD) by the addition of cells.

#### 4.4 Summary

In this chapter, the question was asked whether the EVs can transfer their components to parental cells. Interactions between them was sought by fluorescence microscopy and spectrophotometry with fluorescence probes. Deconvolution fluorescence microscopy opened the possibility of the communication. R18 fluorescence quenching assay provided a definitive observation of the membrane fusion of EVs with the *B. subtilis* cells.

## Chapter 5: Conclusions and perspectives

Two distinctive biological processes, the biogenesis of EVs and formation of spores were studied together in this thesis. Although studies of Gram-positive bacterial EVs were initiated several decades ago, little is known about their biological function. At the start of this research, three major questions were addressed: (1) do *B. subtilis* cells shed EVs during sporulation?; (2) is the proteome of EVs different based on the growth phase?; (3) do the released EVs interact with parental *B. subtilis* cells?

In regard to the first question, EVs were collected from sporulating cells in amounts comparable to EVs from vegetative cells. This observation demonstrated that EV biogenesis by *B. subtilis* is an on-going process, which occurs during sporulation, as well as during vegetative growth. The cell growth conditions and EV isolation procedure were optimized using sequential ultracentrifugation with several filtering steps. TEM analysis showed that the two EV populations were distributed in a similar size range. The EV purification steps could be further optimized based on the purposes of analysis. Especially for therapeutic applications of EVs, methods for obtaining extremely high purity as well as precise evaluation are required. In addition, classification of bacterial EVs based on their sizes might be implemented, because functions and shedding mechanisms of eukaryotic EVs have been considered to differ depending on their sizes.<sup>2</sup>

The second question was addressed in the third chapter on proteomic analysis. EVs from sporulating cells were shown to contain a quantitatively different proteome pattern relative to that from vegetative EVs, even though they share a substantial

number of proteins. The proteins from sporulating EVs showed higher relevance to biological processes contributing to cellular differentiation, while proteins from vegetative EVs are mainly annotated for metabolic processes. More importantly, several proteins abundant in sporulating EVs are known to kill other bacterial species and others participate directly in sporulation. The results suggest that the proteins carried by *B. subtilis* EVs reflect the growth stages of parental cells and environmental stressors. These EV proteins are proposed to support developmental processes including sporulation and bacterial survival. MS-based proteomics analysis is generally composed of several steps including peptide / protein sample preparation, separation, MS analysis, protein identification / scoring, and quantification. Diverse methods at each step have been developed and they result in a number of combinations for an analysis. Multipronged approaches to study the EV proteome using different MS-based methods will enrich our knowledge of the EVs.

Information about transfer pathways of EV contents to Gram-positive bacterial cells was needed to understand the roles of protein cargo in EVs. In chapter 4, we tested the most plausible mechanism, membrane fusion. The spectrophotometric fluorescence de-quenching experiment showed a fusion-like event between EVs and cellular membranes of *B. subtilis* cells. This result supports the proposed function of EVs in intercellular communication. Considering the sporulation-associated proteins identified in EVs and the observed interaction between EVs and *B. subtilis* cells together, it may be assumed that EVs from sporulating bacteria promote further spore formation by delivering relevant proteins to neighboring *B. subtilis* cells.

The studies presented in this thesis are expected to broaden the understanding of Gram-positive bacterial EVs and their relationship with sporulation. Additionally, these observations open further questions such as: (1) are the proteins in EVs biologically active?; (2) how do EVs affect the sporulation process?; (3) could the *B. subtilis* EVs interrupt growth of other bacteria? Based on the present work, future biological research addressing these questions will support applications of the EVs shed by sporulating *B. subtilis* to regulate bacterial sporulation and to strengthen anti-bacterial strategy.



## Appendix

**Appendix table 1.** Proteins identified in vegetative EVs and sporulating EVs (distinct peptides  $\geq 2$ , PSM FDR < 5%, FDR-corrected p-value  $\leq 0.05$ )

Uniprot Accession	Proteins from vegetative EVs			Proteins from sporulating EVs			Rsc (sporulating versus vegetative)	FDR-corrected p-value	Description
	Unique peptides	Sequence coverage	Fisher p-value	Unique peptides	Sequence coverage	Fisher p-value			
Q04789	36	76.67	7.52E-10	2	4.74	5.46E-67	-6.00	1.66E-44	Acetolactate synthase
P94521	24	75.35	3.71E-10	2	5.81	1.22E-49	-5.25	4.94E-34	Putative aminopeptidase YsdC
P39751	16	51.65	5.84E-10	1	2.7	3.81E-14	-4.39	1.78E-10	MreB-like protein
P21881	92	83.56	3.71E-10	40	64.42	0.00E+00*	-4.24	0.00E+00*	Pyruvate dehydrogenase E1 component subunit alpha
P19582	21	51.27	5.84E-10	1	4.16	2.17E-12	-4.22	2.53E-09	Homoserine dehydrogenase
P11998	21	90.91	5.84E-10	12	51.3	1.77E-35	-4.17	8.46E-26	6,7-dimethyl-8-ribityllumazine synthase

O07603	20	54.34	6.35E-10	2	4.62	4.93E-25	-4.12	2.16E-18	Putative aminopeptidase YhfE
O34866	16	69.23	7.57E-10	1	2.56	2.43E-14	-3.99	7.01E-11	Putative carboxypeptidase YodJ
P26900	21	64.44	6.41E-10	4	2.04	2.07E-34	-3.85	1.68E-25	L-asparaginase 1
P80879	13	68.97	6.59E-10	13	71.72	1.21E-14	-3.71	2.72E-11	General stress protein 20U
P40924	8	52.79	2.74E-08	1	2.03	2.67E-08	-3.63	2.58E-06	Phosphoglycerate kinase
P45694	9	47.68	7.24E-10	2	3.45	2.79E-10	-3.57	3.91E-08	Transketolase
P28598	102	92.65	7.95E-10	2	2.94	0.00E+00*	-3.45	1.28E-247	60 kDa chaperonin
O32106	11	58.8	4.16E-07	1	5.2	4.15E-07	-3.43	1.58E-05	Probable cytosol aminopeptidase
P05653	17	50.3	2.24E-10	5	7.43	5.92E-23	-3.39	1.05E-17	DNA gyrase subunit A
P42974	12	54.22	9.20E-07	1	1.77	9.19E-07	-3.36	2.67E-05	NADH dehydrogenase
P37870	13	49.12	5.07E-08	2	3.1	5.06E-08	-3.21	2.80E-06	DNA-directed RNA polymerase subunit beta
P46911	1	14.79	7.43E-08	2	20.36	7.43E-08	-3.18	3.61E-06	Menaquinol-cytochrome c reductase iron-sulfur subunit
Q02112	5	55.88	6.50E-06	1	1.57	6.50E-06	-3.18	1.01E-04	Membrane-bound protein LytA
P55910	9	52.5	1.82E-09	2	13.49	1.36E-09	-2.96	1.24E-07	L-lactate permease
P26901	24	40.79	6.49E-05	1	1.66	6.49E-05	-2.94	4.81E-04	Vegetative catalase
P09124	27	74.03	3.32E-06	2	5.37	3.32E-06	-2.90	4.88E-05	Glyceraldehyde-3-phosphate dehydrogenase 1

C0SP94	18	42.41	9.52E-05	1	2.79	9.52E-05	-2.89	6.24E-04	Putative ABC transporter substrate-binding lipoprotein YhfQ
P37941	8	47.4	2.95E-05	1	9.48	2.95E-05	-2.69	2.33E-04	2-oxoisovalerate dehydrogenase subunit beta
P94356	27	87.78	6.57E-10	15	47.78	8.31E-36	-2.65	6.94E-29	Uncharacterized protein YxkC
P96499	19	35.04	8.90E-04	1	3.07	8.90E-04	-2.58	3.25E-03	Putative transcriptional regulator YvhJ
P21882	100	84.92	7.66E-10	23	59.38	0.00E+00*	-2.54	0.00E+00*	Pyruvate dehydrogenase E1 component subunit beta
P54326	8	49.82	1.88E-03	1	7.14	1.88E-03	-2.47	5.56E-03	Phage-like element PBSX protein XkdF
P13243	20	70.88	4.59E-07	2	5.96	4.59E-07	-2.46	7.36E-06	Probable fructose-bisphosphate aldolase
P39594	2	10.36	8.94E-08	2	11.7	8.90E-08	-2.43	2.01E-06	Thiamine-phosphate synthase
P19669	26	81.6	2.47E-07	1	3.77	2.47E-07	-2.37	4.20E-06	Transaldolase
O34594	9	71.43	9.72E-06	1	7.25	9.72E-06	-2.24	7.22E-05	Cytochrome c-551
P12425	65	85.14	6.59E-10	27	71.85	0.00E+00*	-2.15	2.50E-246	Glutamine synthetase
P40409	10	30.91	1.38E-04	2	3.15	1.38E-04	-2.14	5.66E-04	Iron-uptake system-binding protein
P21880	98	89.57	3.71E-10	77	36.8	0.00E+00*	-2.08	0.00E+00*	Dihydrolipoyl dehydrogenase
P71017	2	6.11	1.66E-02	1	9.95	1.66E-02	-2.03	2.77E-02	Alcohol dehydrogenase

O32218	23	67.12	2.76E-08	17	59.01	2.68E-08	-2.02	4.58E-07	Disulfide bond formation protein D
O34385	9	63.4	5.81E-06	1	2.61	5.81E-06	-1.98	3.87E-05	Manganese-binding lipoprotein MntA
O32167	20	79.56	2.73E-09	4	13.14	2.35E-09	-1.97	5.35E-08	Methionine-binding lipoprotein MetQ
P13242	8	41.12	9.76E-03	3	9.16	9.76E-03	-1.72	1.73E-02	CTP synthase
P80861	16	57.4	1.18E-08	2	4.59	1.15E-08	-1.69	1.49E-07	NADH dehydrogenase-like protein YjID
P39793	35	57.77	5.93E-10	11	27.5	3.27E-13	-1.68	7.74E-12	Penicillin-binding protein 1A/1B
O34633	18	94.29	7.52E-10	12	75	5.34E-27	-1.62	7.86E-24	Uncharacterized protein YjIC
P37580	9	36.83	3.66E-10	1	6.98	2.24E-12	-1.61	3.64E-11	Iron(3+)-hydroxamate-binding protein FhuD
P54531	14	58.79	2.03E-06	1	2.75	2.03E-06	-1.58	1.17E-05	Leucine dehydrogenase
P37527	20	67.35	4.23E-08	5	23.47	4.19E-08	-1.49	3.82E-07	Pyridoxal biosynthesis lyase PdxS
P80244	2	13.2	3.10E-02	1	4.06	3.10E-02	-1.48	4.41E-02	ATP-dependent Clp protease proteolytic subunit
O34916	4	14.44	3.16E-02	3	6.42	3.16E-02	-1.36	4.56E-02	N-acetyldiaminopimelate deacetylase
P21883	98	85.29	4.62E-10	87	78.51	1.34E-304	-1.35	3.66E-245	Dihydrolipoyllysine-residue acetyltransferase component of pyruvate dehydrogenase complex

P94428	5	24.46	1.44E-03	2	3.46	1.44E-03	-1.35	3.32E-03	Succinate-semialdehyde dehydrogenase [NADP(+)]
P94541	19	49.2	2.77E-05	2	9.9	2.77E-05	-1.20	9.24E-05	Ribonuclease HIII
P50849	20	50.5	1.64E-04	4	6.52	1.64E-04	-1.11	4.30E-04	Polyribonucleotide nucleotidyltransferase
P13714	40	80.31	9.57E-03	34	77.5	9.57E-03	-0.90	1.65E-02	L-lactate dehydrogenase
P54423	85	63.87	3.52E-09	23	49.11	2.74E-09	-0.38	1.40E-08	Cell wall-associated protease
P40767	5	12.9	5.12E-01	5	13.32	5.12E-01	-0.18	4.90E-02	Peptidoglycan DL-endopeptidase CwIO
P39645	7	45.67	2.85E-02	2	5.91	2.85E-02	0.35	4.27E-02	Putative heme-dependent peroxidase YwfI
O34788	13	65.9	6.50E-06	8	17.05	6.50E-06	0.72	7.09E-06	(R,R)-butanediol dehydrogenase
P94431	3	22.55	9.49E-03	10	35.78	9.49E-03	0.78	1.16E-02	Uncharacterized protein YcnI
P54331	1	1.72	7.87E-04	5	13.52	7.87E-04	0.85	8.61E-04	Phage-like element PBSX protein XkdK
O34575	48	46.51	5.57E-16	45	42.63	1.01E-09	0.92	1.46E-16	Putative mannosyltransferase YkcB
P08838	12	46.67	1.27E-05	2	6.84	1.27E-05	0.94	1.17E-05	Phosphoenolpyruvate-protein phosphotransferase
P39215	2	7.4	4.11E-03	3	6.95	4.11E-03	1.13	4.11E-03	Methyl-accepting chemotaxis protein McpB

Q08352	11	51.32	1.13E-04	27	72.49	1.13E-04	1.27	9.14E-05	Alanine dehydrogenase
O32101	2	5.48	2.92E-02	5	29.18	2.92E-02	1.29	2.90E-02	Bacteriophage SPP1 adsorption protein YueB
Q45493	33	80.18	4.76E-29	23	67.75	8.88E-10	1.42	1.18E-30	Ribonuclease J1
Q02114	1	4.64	3.72E-01	2	4.84	3.72E-01	1.44	3.33E-02	N-acetylmuramoyl-L-alanine amidase LytC
P42971	26	59.58	3.53E-26	7	3.74	8.17E-10	1.60	9.13E-28	Penicillin-binding protein 3
P42297	3	15.54	4.94E-04	4	22.97	4.94E-04	1.62	3.45E-04	Universal stress protein YxiE
P54608	5	7.6	2.67E-02	3	3.51	2.67E-02	1.66	2.21E-02	Hydrolase YhcX
P20282	2	12.4	4.98E-02	6	42.98	4.98E-02	1.72	4.25E-02	30S ribosomal protein S13
P37871	3	3.67	4.98E-02	2	1.25	4.98E-02	1.72	4.25E-02	DNA-directed RNA polymerase subunit beta'
O32052	2	21.35	2.74E-02	4	64.04	2.74E-02	1.75	2.20E-02	UPF0092 membrane protein YrbF
P32399	5	7.35	1.26E-08	3	3.23	1.30E-08	1.83	4.54E-09	Uncharacterized protein YhgE
P39214	3	13.31	2.27E-49	3	11.19	8.55E-10	1.91	2.47E-52	Methyl-accepting chemotaxis protein McpA
P17820	3	7.34	3.80E-03	4	9	3.80E-03	1.98	2.57E-03	Chaperone protein DnaK
Q01466	5	26.21	2.72E-02	22	51.38	2.72E-02	2.03	1.92E-02	Cell shape-determining protein MreC
P33166	11	32.57	9.37E-29	9	15.4	8.17E-10	2.06	1.31E-30	Elongation factor Tu

P16524	23	59.29	2.83E-09	31	67.94	2.93E-09	2.07	8.35E-10	Putative N-acetyl-LL-diaminopimelate aminotransferase
P42175	20	60.1	2.95E-41	17	54.15	5.41E-10	2.13	9.12E-44	Nitrate reductase alpha chain
P40403	2	23.44	1.18E-45	3	27.75	8.17E-10	2.17	2.11E-48	CheY-P phosphatase CheC
P34957	10	32.4	9.46E-26	5	9.35	7.73E-10	2.18	2.02E-27	Quinol oxidase subunit 2
P42176	10	25.05	1.28E-26	8	14.78	7.88E-10	2.19	2.40E-28	Nitrate reductase beta chain
O31560	7	39.51	7.72E-06	7	27.8	7.72E-06	2.32	3.70E-06	Uncharacterized HTH-type transcriptional regulator YfiR
Q07833	2	1.33	2.03E-06	6	5.1	2.03E-06	2.33	8.96E-07	tRNA nuclease WapA
O34790	1	7.02	4.46E-02	8	45.18	4.46E-02	2.38	2.80E-02	Heptaprenylglyceryl phosphate synthase
O34847	1	4.31	4.46E-02	11	43.38	4.46E-02	2.38	2.80E-02	Acetyl-coenzyme A carboxylase carboxyl transferase subunit alpha
P0CI78	2	16.5	4.46E-02	6	40.78	4.46E-02	2.38	2.80E-02	50S ribosomal protein L24
P39606	2	6.01	1.16E-02	2	6.01	1.16E-02	2.41	6.75E-03	Uncharacterized protein YwcH
P71019	1	9.78	2.07E-02	2	9.78	2.07E-02	2.59	1.16E-02	Malonyl CoA-acyl carrier protein transacylase
P42400	5	24.74	3.91E-21	3	14.63	8.17E-10	2.64	1.93E-22	Probable ABC transporter extracellular-binding protein YckB

P50727	1	15.85	5.58E-04	8	48.78	5.58E-04	2.65	2.93E-04	Ferredoxin
O34340	0	0	8.06E-02	16	51.57	8.06E-02	2.67	3.72E-02	3-oxoacyl-[acyl-carrier-protein] synthase 2
O34353	0	0	8.06E-02	8	25.57	8.06E-02	2.67	3.72E-02	Uncharacterized protein YdjN
P39623	0	0	8.06E-02	2	7.97	8.06E-02	2.67	3.72E-02	Spore coat polysaccharide biosynthesis protein SpsC
P50829	0	0	8.06E-02	11	39.88	8.06E-02	2.67	3.72E-02	Putative phosphotransferase enzyme IIA component YpqE
P54459	0	0	8.06E-02	3	7.78	8.06E-02	2.67	3.72E-02	Uncharacterized protein YqeN
P54956	0	0	8.06E-02	12	30.79	8.06E-02	2.67	3.72E-02	Uncharacterized protein YxeQ
P70974	0	0	8.06E-02	2	12.41	8.06E-02	2.67	3.72E-02	50S ribosomal protein L13
Q01465	0	0	8.06E-02	15	44.51	8.06E-02	2.67	3.72E-02	Rod shape-determining protein MreB
P54341	6	14.08	5.20E-111	16	45.12	7.73E-10	2.68	2.19E-116	Phage-like element PBSX protein XkdV
P02394	2	19.51	9.02E-04	8	26.83	9.02E-04	2.82	4.73E-04	50S ribosomal protein L7/L12
P54375	2	13.86	1.97E-08	6	38.61	1.99E-08	2.87	7.01E-09	Superoxide dismutase [Mn]
P37809	37	61.95	1.08E-85	51	76.74	7.88E-10	2.88	1.25E-89	ATP synthase subunit beta



P37808	27	53.78	4.08E-96	50	67.93	7.55E-10	2.97	3.36E-100	ATP synthase subunit alpha
O07543	0	0	3.16E-02	10	23.87	3.16E-02	2.98	1.47E-02	UPF0754 membrane protein YheB
O34645	0	0	3.16E-02	9	24.77	3.16E-02	2.98	1.47E-02	Alpha-galactosidase
P16263	0	0	3.16E-02	36	71.46	3.16E-02	2.98	1.47E-02	Dihydrolipoyllysine-residue succinyltransferase component of 2-oxoglutarate dehydrogenase complex
P51834	0	0	3.16E-02	3	3.12	3.16E-02	2.98	1.47E-02	Chromosome partition protein Smc
P96681	0	0	3.16E-02	20	43.15	3.16E-02	2.98	1.47E-02	Uncharacterized HTH-type transcriptional regulator YdfD
Q45585	0	0	3.16E-02	5	23.53	3.16E-02	2.98	1.47E-02	ECF RNA polymerase sigma factor SigW
O34841	1	7.18	1.63E-04	3	9.39	1.63E-04	3.04	8.26E-05	Uncharacterized protein YoeB
Q45584	1	4.64	1.40E-03	6	39.07	1.40E-03	3.09	6.95E-04	Uncharacterized protein YbbK
P39216	3	9.52	2.42E-47	3	7.4	1.03E-09	3.12	2.42E-49	Methyl-accepting chemotaxis protein TlpA
O05389	0	0	1.23E-02	2	4.99	1.23E-02	3.23	5.56E-03	Uncharacterized oxidoreductase YrbE
O07610	0	0	1.23E-02	2	4.29	1.23E-02	3.23	5.56E-03	Long-chain-fatty-acid-CoA ligase
O32100	0	0	1.23E-02	7	64.9	1.23E-02	3.23	5.56E-03	Uncharacterized protein YueC

P13267	0	0	1.23E-02	3	2.99	1.23E-02	3.23	5.56E-03	DNA polymerase III PolC-type
P54567	0	0	1.23E-02	6	19.67	1.23E-02	3.23	5.56E-03	Uncharacterized protein YqkD
P94367	0	0	1.23E-02	11	20.17	1.23E-02	3.23	5.56E-03	ATP-binding/permease protein CydD
P12875	1	7.38	5.63E-04	21	68.03	5.63E-04	3.23	2.87E-04	50S ribosomal protein L14
P42100	1	9.16	5.63E-04	2	11.78	5.63E-04	3.23	2.87E-04	Glycerate kinase
P0CI74	7	55.1	1.07E-13	7	28.57	8.17E-10	3.29	2.05E-14	Cell cycle protein GpsB
O31529	2	3.32	1.11E-05	2	4.83	1.11E-05	3.31	5.56E-06	Beta-galactosidase YesZ
P54602	4	4.93	4.88E-75	19	67.38	9.95E-10	3.34	1.74E-77	Endonuclease YhcR
O32023	3	27.27	2.23E-04	7	44.16	2.23E-04	3.35	1.13E-04	Uncharacterized protein YqzC
P96583	3	4.26	2.23E-04	2	3.3	2.23E-04	3.35	1.13E-04	DNA topoisomerase 3
P80698	4	15.8	1.21E-15	8	18.87	6.04E-10	3.43	2.39E-16	Trigger factor
P54334	4	5.48	1.98E-09	4	3.3	2.53E-09	3.43	8.01E-10	Phage-like element PBSX protein XkdO
O34309	0	0	4.60E-03	3	3.35	4.60E-03	3.44	2.18E-03	Putative phosphoenolpyruvate synthase
P08065	0	0	4.60E-03	2	3.58	4.60E-03	3.44	2.18E-03	Succinate dehydrogenase flavoprotein subunit
O31760	14	48.83	9.63E-163	30	74.23	7.88E-10	3.54	3.66E-32	Ribonuclease J2
O07021	1	4.18	7.47E-11	3	4.18	2.89E-10	3.61	2.24E-11	Lactate utilization protein B
O35000	0	0	1.66E-03	14	50.83	1.66E-03	3.63	8.16E-04	Glucosamine-6- phosphate deaminase 1

P53001	1	2.8	1.32E-05	3	8.91	1.32E-05	3.67	7.30E-06	Aspartate aminotransferase
P24136	1	3.07	5.22E-06	2	5.87	5.22E-06	3.76	2.97E-06	Oligopeptide transport ATP-binding protein OppD
Q45597	3	6.55	1.45E-14	4	5.77	8.17E-10	3.76	4.34E-15	Fructose-1,6-bisphosphatase class 3
P71012	2	5.51	2.57E-23	3	10.71	7.88E-10	3.76	5.97E-24	PTS system fructose-specific EIIABC component
O31927	0	0	6.06E-04	30	3.89	6.06E-04	3.79	3.23E-04	SPBc2 prophage-derived uncharacterized protein YopK
O32072	0	0	6.06E-04	14	70.87	6.06E-04	3.79	3.23E-04	Uncharacterized protein YtwF
P37471	0	0	6.06E-04	7	44	6.06E-04	3.79	3.23E-04	Cell division protein DivIC
P54327	17	77.81	0.00E+00*	48	89.71	7.88E-10	3.93	0.00E+00*	Phage-like element PBSX protein XkdG
P30949	0	0	2.23E-04	2	4.88	2.23E-04	3.94	1.26E-04	Glutamate-1-semialdehyde 2,1-aminomutase
P54340	0	0	2.23E-04	12	35.94	2.23E-04	3.94	1.26E-04	Phage-like element PBSX protein XkdU
P17904	0	0	8.27E-05	8	52.5	8.27E-05	4.08	5.09E-05	Serine-protein kinase RsbW
P0CI73	1	2.33	4.02E-08	5	5.67	4.06E-08	4.15	2.84E-08	Glutamine--fructose-6-phosphate aminotransferase [isomerizing]

P39456	0	0	2.95E-05	2	10.12	2.95E-05	4.20	1.97E-05	L-cystine import ATP-binding protein TcyC
P54560	0	0	2.95E-05	3	5.83	2.95E-05	4.20	1.97E-05	DNA polymerase IV 2
P55873	0	0	2.95E-05	10	54.62	2.95E-05	4.20	1.97E-05	50S ribosomal protein L20
P45921	5	25.4	1.17E-101	34	45.6	7.88E-10	4.21	1.12E-101	Uncharacterized protein YqbE
P21464	13	47.97	7.48E-195	43	77.64	7.55E-10	4.23	6.10E-194	30S ribosomal protein S2
P71021	4	28.05	1.25E-36	5	23.78	9.07E-10	4.40	1.46E-36	Septum site-determining protein DivIVA
P24137	1	2.3	2.30E-11	3	8.85	7.88E-10	4.61	1.76E-11	Oligopeptide transport ATP-binding protein OppF
O31740	0	0	1.84E-07	15	47.7	1.85E-07	4.69	1.87E-07	Ribosome maturation factor RimM
P54339	7	29.02	6.10E-122	16	54.6	9.95E-10	4.83	3.43E-119	Phage-like element PBSX protein XkdT
P94421	8	25.87	1.32E-41	22	40.69	7.55E-10	4.85	8.02E-41	Uncharacterized ABC transporter solute-binding protein YclQ
O34662	0	0	2.46E-08	2	3.38	2.53E-08	4.85	2.90E-08	Uncharacterized aminotransferase YodT
P21467	0	0	2.46E-08	27	56.63	2.53E-08	4.85	2.90E-08	30S ribosomal protein S5
P20166	3	7.15	6.56E-38	6	11.79	7.55E-10	4.91	3.96E-37	PTS system glucose-specific EIICBA component

Q06796	0	0	9.03E-09	10	55.32	9.17E-09	4.92	1.16E-08	50S ribosomal protein L11
Q45596	0	0	9.03E-09	6	71.43	9.17E-09	4.92	1.16E-08	Putative exported peptide YydF
O32258	1	3.2	9.25E-16	4	4.94	7.88E-10	5.03	1.50E-15	Uncharacterized glycosylase YvbX
P46898	1	6.7	4.49E-17	17	62.57	7.88E-10	5.14	9.35E-17	50S ribosomal protein L6
P05657	0	0	2.14E-10	2	9.57	8.17E-10	5.18	2.78E-10	50S ribosomal protein L27
P21475	0	0	2.14E-10	5	30.38	8.17E-10	5.18	2.78E-10	30S ribosomal protein S18
P28628	0	0	7.71E-11	14	61.41	7.88E-10	5.24	1.11E-10	Signal peptidase I S
P54332	3	20.41	7.76E-74	3	29.25	2.89E-10	5.28	3.38E-71	Phage-like element PBSX protein XkdM
P54507	0	0	2.78E-11	3	6.9	7.73E-10	5.30	4.37E-11	Spore coat-associated protein N
O34450	2	9.34	1.23E-20	10	34.09	8.17E-10	5.39	5.26E-20	N-acetylglucosamine-6-phosphate deacetylase
P04969	0	0	3.50E-12	6	37.4	8.17E-10	5.40	7.04E-12	30S ribosomal protein S11
Q45598	0	0	3.50E-12	3	3.24	8.17E-10	5.40	7.04E-12	Uncharacterized protein YydD
O31550	20	31.16	2.45E-64	20	41.46	0.00E+00*	5.41	8.34E-62	Dihydrolipoyllysine-residue acetyltransferase component of acetoin cleaving system
P42060	0	0	1.90E-14	6	37.17	8.52E-10	5.64	6.28E-14	50S ribosomal protein L22

P54325	4	27.68	7.72E-109	8	49.9	3.82E-10	5.65	1.35E-103	Phage-like element PBSX protein XkdE
P40406	0	0	1.08E-16	4	6.39	1.87E-10	5.84	5.87E-16	Beta-hexosaminidase
P19946	0	0	2.49E-20	2	8.22	7.88E-10	6.12	3.36E-19	50S ribosomal protein L15
P12877	1	5.03	9.98E-42	16	50.84	7.88E-10	6.34	4.74E-39	50S ribosomal protein L5
P46899	0	0	2.49E-25	2	7.5	9.29E-11	6.42	1.12E-23	50S ribosomal protein L18
O34469	1	1.33	3.53E-61	3	3.84	1.76E-10	6.87	1.85E-56	Putative ATP- dependent helicase YeeB
O31742	0	0	6.89E-35	7	46.96	4.37E-10	6.88	3.66E-32	50S ribosomal protein L19
P19405	1	1.95	6.81E-69	7	32.68	7.61E-10	7.04	2.34E-63	Alkaline phosphatase 3
P21473	0	0	1.04E-46	7	41.57	3.33E-10	7.29	1.01E-42	30S ribosomal protein S15
P26908	0	0	2.10E-49	8	52.94	7.88E-10	7.37	3.95E-45	50S ribosomal protein L21
P42919	0	0	1.73E-59	3	8.66	7.73E-10	7.64	4.76E-54	50S ribosomal protein L2
P21469	0	0	2.59E-82	11	39.1	4.44E-10	8.10	2.38E-74	30S ribosomal protein S7
P21466	4	22	2.22E-193	20	65	7.55E-10	8.50	7.48E-174	30S ribosomal protein S4

\* p-values of 0.00E+00 represent the values < 2.2E-308.

## Bibliography

- (1) Deatherage, B. L.; Cookson, B. T. Membrane Vesicle Release in Bacteria, Eukaryotes, and Archaea: A Conserved yet Underappreciated Aspect of Microbial Life. *Infect. Immun.* **2012**, *80* (6), 1948–1957.
- (2) Raposo, G.; Stoorvogel, W. Extracellular Vesicles: Exosomes, Microvesicles, and Friends. *J. Cell Biol.* **2013**, *200* (4), 373–383.
- (3) Andaloussi, S. E.; Mäger, I.; Breakefield, X. O.; Wood, M. J. A. Extracellular Vesicles: Biology and Emerging Therapeutic Opportunities. *Nat. Rev. Drug Discov.* **2013**, *12* (5), 347–357.
- (4) Bishop, D. G.; Work, E. An Extracellular Glycolipid Produced by *Escherichia coli* Grown under Lysine-Limiting Conditions. *Biochem. J.* **1965**, *96* (2), 567–576.
- (5) Kulp, A.; Kuehn, M. J. Biological Functions and Biogenesis of Secreted Bacterial Outer Membrane Vesicles. *Annu. Rev. Microbiol.* **2010**, *64*, 163–184.
- (6) Brown, L.; Kessler, A.; Cabezas-Sanchez, P.; Luque-Garcia, J. L.; Casadevall, A. Extracellular Vesicles Produced by the Gram-Positive Bacterium *Bacillus subtilis* Are Disrupted by the Lipopeptide Surfactin. *Mol. Microbiol.* **2014**, *93* (1), 183–198.
- (7) Lee, E.-Y.; Choi, D.-Y.; Kim, D.-K.; Kim, J.-W.; Park, J. O.; Kim, S.; Kim, S.-H.; Desiderio, D. M.; Kim, Y.-K.; Kim, K.-P.; et al. Gram-Positive Bacteria Produce Membrane Vesicles: Proteomics-Based Characterization of *Staphylococcus aureus*-Derived Membrane Vesicles. *Proteomics* **2009**, *9* (24), 5425–5436.
- (8) Kuehn, M. J.; Kesty, N. C. Bacterial Outer Membrane Vesicles and the Host-Pathogen Interaction. *Genes Dev.* **2005**, *19* (22), 2645–2655.
- (9) Lee, E.-Y.; Choi, D.-S.; Kim, K.-P.; Gho, Y. S. Proteomics in Gram-Negative Bacterial Outer Membrane Vesicles. *Mass Spectrom. Rev.* **2008**, *27* (6), 535–555.
- (10) Ellis, T. N.; Leiman, S. A.; Kuehn, M. J. Naturally Produced Outer Membrane Vesicles from *Pseudomonas aeruginosa* Elicit a Potent Innate Immune

- Response via Combined Sensing of Both Lipopolysaccharide and Protein Components. *Infect. Immun.* **2010**, 78 (9), 3822–3831.
- (11) Mashburn, L. M.; Whiteley, M. Membrane Vesicles Traffic Signals and Facilitate Group Activities in a Prokaryote. *Nature* **2005**, 437 (7057), 422–425.
  - (12) Dubern, J.-F.; Diggle, S. P. Quorum Sensing by 2-Alkyl-4-Quinolones in *Pseudomonas aeruginosa* and Other Bacterial Species. *Mol. Biosyst.* **2008**, 4 (9), 882–888.
  - (13) Deatherage, B. L.; Lara, J. C.; Bergsbaken, T.; Rassouljian Barrett, S. L.; Lara, S.; Cookson, B. T. Biogenesis of Bacterial Membrane Vesicles. *Mol. Microbiol.* **2009**, 72 (6), 1395–1407.
  - (14) McBroom, A. J.; Kuehn, M. J. Release of Outer Membrane Vesicles by Gram-Negative Bacteria Is a Novel Envelope Stress Response. *Mol. Microbiol.* **2007**, 63 (2), 545–558.
  - (15) Kadurugamuwa, J. L.; Beveridge, T. J. Bacteriolytic Effect of Membrane Vesicles from *Pseudomonas aeruginosa* on Other Bacteria Including Pathogens: Conceptually New Antibiotics. *J. Bacteriol.* **1996**, 178 (10), 2767–2774.
  - (16) Vasilyeva, N. V; Tsfasman, I. M.; Suzina, N. E.; Stepnaya, O. A.; Kulaev, I. S. Secretion of Bacteriolytic Endopeptidase L5 of *Lysobacter* Sp. XL1 into the Medium by Means of Outer Membrane Vesicles. *FEBS J.* **2008**, 275 (15), 3827–3835.
  - (17) Schooling, S. R.; Beveridge, T. J. Membrane Vesicles: An Overlooked Component of the Matrices of Biofilms. *J. Bacteriol.* **2006**, 188 (16), 5945–5957.
  - (18) Yonezawa, H.; Osaki, T.; Kurata, S.; Fukuda, M.; Kawakami, H.; Ochiai, K.; Hanawa, T.; Kamiya, S. Outer Membrane Vesicles of *Helicobacter pylori* TK1402 Are Involved in Biofilm Formation. *BMC Microbiol.* **2009**, 9, 197.
  - (19) Gankema, H.; Wensink, J.; Guinée, P. A.; Jansen, W. H.; Witholt, B. Some Characteristics of the Outer Membrane Material Released by Growing Enterotoxigenic *Escherichia coli*. *Infect. Immun.* **1980**, 29 (2), 704–713.
  - (20) Kato, S.; Kowashi, Y.; Demuth, D. R. Outer Membrane-like Vesicles Secreted by *Actinobacillus actinomycetemcomitans* Are Enriched in Leukotoxin. *Microb. Pathog.* **2002**, 32 (1), 1–13.
  - (21) Rivera, J.; Cordero, R. J. B.; Nakouzi, A. S.; Frases, S.; Nicola, A.; Casadevall, A. *Bacillus anthracis* Produces Membrane-Derived Vesicles Containing



- Biologically Active Toxins. *Proc. Natl. Acad. Sci. U. S. A.* **2010**, *107* (44), 19002–19007.
- (22) Ellis, T. N.; Kuehn, M. J. Virulence and Immunomodulatory Roles of Bacterial Outer Membrane Vesicles. *Microbiol. Mol. Biol. Rev.* **2010**, *74* (1), 81–94.
- (23) Lam, M. Y.; McGroarty, E. J.; Kropinski, A. M.; MacDonald, L. A.; Pedersen, S. S.; Høiby, N.; Lam, J. S. Occurrence of a Common Lipopolysaccharide Antigen in Standard and Clinical Strains of *Pseudomonas aeruginosa*. *J. Clin. Microbiol.* **1989**, *27* (5), 962–967.
- (24) Rivera, M.; Bryan, L. E.; Hancock, R. E.; McGroarty, E. J. Heterogeneity of Lipopolysaccharides from *Pseudomonas aeruginosa*: Analysis of Lipopolysaccharide Chain Length. *J. Bacteriol.* **1988**, *170* (2), 512–521.
- (25) Nguyen, T. T.; Saxena, A.; Beveridge, T. J. Effect of Surface Lipopolysaccharide on the Nature of Membrane Vesicles Liberated from the Gram-Negative Bacterium *Pseudomonas aeruginosa*. *J. Electron Microsc. (Tokyo)*. **2003**, *52* (5), 465–469.
- (26) Van de Waterbeemd, B.; Streefland, M.; van der Ley, P.; Zomer, B.; van Dijken, H.; Martens, D.; Wijffels, R.; van der Pol, L. Improved OMV Vaccine against *Neisseria meningitidis* Using Genetically Engineered Strains and a Detergent-Free Purification Process. *Vaccine* **2010**, *28* (30), 4810–4816.
- (27) Collins, B. S. Gram-Negative Outer Membrane Vesicles in Vaccine Development. *Discov. Med.* **2011**, *12* (62), 7–15.
- (28) Feiring, B.; Fuglesang, J.; Oster, P.; Naess, L. M.; Helland, O. S.; Tilman, S.; Rosenqvist, E.; Bergsaker, M. A. R.; Nøkleby, H.; Aaberge, I. S. Persisting Immune Responses Indicating Long-Term Protection after Booster Dose with Meningococcal Group B Outer Membrane Vesicle Vaccine. *Clin. Vaccine Immunol.* **2006**, *13* (7), 790–796.
- (29) Jackson, C.; Lennon, D. R.; Sotutu, V. T. K.; Yan, J.; Stewart, J. M.; Reid, S.; Crengle, S.; Oster, P.; Ypma, E.; Aaberge, I.; et al. Phase II Meningococcal B Vesicle Vaccine Trial in New Zealand Infants. *Arch. Dis. Child.* **2009**, *94* (10), 745–751.
- (30) Holst, J.; Martin, D.; Arnold, R.; Huergo, C. C.; Oster, P.; O’Hallahan, J.; Rosenqvist, E. Properties and Clinical Performance of Vaccines Containing Outer Membrane Vesicles from *Neisseria meningitidis*. *Vaccine* **2009**, *27* Suppl 2, B3–B12.

- (31) Dorward, D. W.; Garon, C. F. DNA Is Packaged within Membrane-Derived Vesicles of Gram-Negative but Not Gram-Positive Bacteria. *Appl. Environ. Microbiol.* **1990**, *56* (6), 1960–1962.
- (32) Gurung, M.; Moon, D. C.; Choi, C. W.; Lee, J. H.; Bae, Y. C.; Kim, J.; Lee, Y. C.; Seol, S. Y.; Cho, D. T.; Kim, S. Il; et al. *Staphylococcus aureus* Produces Membrane-Derived Vesicles That Induce Host Cell Death. *PLoS One* **2011**, *6* (11), e27958.
- (33) Lee, J. H.; Choi, C.-W.; Lee, T.; Kim, S. Il; Lee, J.-C.; Shin, J.-H. Transcription Factor  $\sigma$ B Plays an Important Role in the Production of Extracellular Membrane-Derived Vesicles in *Listeria monocytogenes*. *PLoS One* **2013**, *8* (8), e73196.
- (34) Jiang, Y.; Kong, Q.; Roland, K. L.; Curtiss, R. Membrane Vesicles of *Clostridium perfringens* Type A Strains Induce Innate and Adaptive Immunity. *Int. J. Med. Microbiol.* **2014**, *304* (3-4), 431–443.
- (35) Olaya-Abril, A.; Prados-Rosales, R.; McConnell, M. J.; Martín-Peña, R.; González-Reyes, J. A.; Jiménez-Munguía, I.; Gómez-Gascón, L.; Fernández, J.; Luque-García, J. L.; García-Lidón, C.; et al. Characterization of Protective Extracellular Membrane-Derived Vesicles Produced by *Streptococcus pneumoniae*. *J. Proteomics* **2014**, *106*, 46–60.
- (36) Cohn, F. Untersuchungen Über Bakterien I. *Beitr. Biol. Pflanz.* **1875**, *1*, 127–224.
- (37) Fritze, D. Taxonomy of the Genus *bacillus* and Related Genera: The Aerobic Endospore-Forming Bacteria. *Phytopathology* **2004**, *94* (11), 1245–1248.
- (38) Parry, J. M.; Turnbull, P. C. B.; Gibson, J. R. *A Colour Atlas of Bacillus Species.*; Wolfe Medical Publications Ltd: London, 1983.
- (39) Stead, D. E.; Sellwood, J. E.; Wilson, J.; Viney, I. Evaluation of a Commercial Microbial Identification System Based on Fatty Acid Profiles for Rapid, Accurate Identification of Plant Pathogenic Bacteria. *J. Appl. Bacteriol.* **1992**, *72* (4), 315–321.
- (40) Ash, C.; Farrow, J. A.; Dorsch, M.; Stackebrandt, E.; Collins, M. D. Comparative Analysis of *Bacillus anthracis*, *Bacillus cereus*, and Related Species on the Basis of Reverse Transcriptase Sequencing of 16S rRNA. *Int. J. Syst. Bacteriol.* **1991**, *41* (3), 343–346.
- (41) Harwood, C. R.; Archibald, A. R. *Growth, Maintenance and General Techniques*; Harwood, C., Cutting, S., Eds.; John Wiley and Sons: Chichester, England, 1990; pp 1–21.

- (42) Mock, M.; Mignot, T. Anthrax Toxins and the Host: A Story of Intimacy. *Cell. Microbiol.* **2003**, *5* (1), 15–23.
- (43) Mock, M.; Fouet, A. Anthrax. *Annu. Rev. Microbiol.* **2001**, *55*, 647–671.
- (44) Hong, H. A.; Khaneja, R.; Tam, N. M. K.; Cazzato, A.; Tan, S.; Urdaci, M.; Brisson, A.; Gasbarrini, A.; Barnes, I.; Cutting, S. M. *Bacillus subtilis* Isolated from the Human Gastrointestinal Tract. *Res. Microbiol.* **2009**, *160* (2), 134–143.
- (45) Guttenplan, S. B.; Shaw, S.; Kearns, D. B. The Cell Biology of Peritrichous Flagella in *Bacillus subtilis*. *Mol. Microbiol.* **2013**, *87* (1), 211–229.
- (46) Stein, T. *Bacillus subtilis* Antibiotics: Structures, Syntheses and Specific Functions. *Mol. Microbiol.* **2005**, *56* (4), 845–857.
- (47) Kuwana, R.; Kasahara, Y.; Fujibayashi, M.; Takamatsu, H.; Ogasawara, N.; Watabe, K. Proteomics Characterization of Novel Spore Proteins of *Bacillus subtilis*. *Microbiology* **2002**, *148* (12), 3971–3982.
- (48) Errington, J. Regulation of Endospore Formation in *Bacillus subtilis*. *Nat. Rev. Microbiol.* **2003**, *1* (2), 117–126.
- (49) Stragier, P.; Losick, R. Molecular Genetics of Sporulation in *Bacillus subtilis*. *Annu. Rev. Genet.* **1996**, *30*, 297–41.
- (50) Nicholson, W. L.; Setlow, P. Sporulation, Germination, and Outgrowth. In *Molecular Biological Methods for Bacillus*; Harward, C. R., Cutting, S. M., Eds.; John Wiley and Sons: Chichester, England, 1990; pp 391–450.
- (51) Fenselau, C.; Wynne, C.; Edwards, N. Broadband Analysis of Bioagents by Mass Spectrometry. In *Detection of biological agents for the prevention of bioterrorism*; 2011; pp 1–12.
- (52) Setlow, B.; Atluri, S.; Kitchel, R.; Koziol-Dube, K.; Setlow, P. Role of Dipicolinic Acid in Resistance and Stability of Spores of *Bacillus subtilis* with or without DNA-Protective Alpha/beta-Type Small Acid-Soluble Proteins. *J. Bacteriol.* **2006**, *188* (11), 3740–3747.
- (53) Smith, B. W.; Roe, J. H. A Photometric Method for the Determination of Alpha-Amylase in Blood and Urine, with Use of the Starch-Iodine Color. *J. Biol. Chem.* **1949**, *179* (1), 53–59.
- (54) Dancer, B. N.; Mandelstam, J. Production and Possible Function of Serine Protease during Sporulation of *Bacillus subtilis*. *J. Bacteriol.* **1975**, *121* (2), 406–410.

- (55) Glenn, A. R.; Mandelstam, J. Sporulation in *Bacillus subtilis* 168. Comparison of Alkaline Phosphatase from Sporulating and Vegetative Cells. *Biochem. J.* **1971**, *123* (2), 129–138.
- (56) Errington, J.; Mandelstam, J. Use of a lacZ Gene Fusion to Determine the Dependence Pattern of Sporulation Operon spoIIA in Spo Mutants of *Bacillus subtilis*. *J. Gen. Microbiol.* **1986**, *132* (11), 2967–2976.
- (57) Janssen, F. W.; Lund, A. J.; Anderson, L. E. Colorimetric Assay for Dipicolinic Acid in Bacterial Spores. *Science* **1958**, *127* (3288), 26–27.
- (58) Milhaud, P.; Balassa, G. Biochemical Genetics of Bacterial Sporulation. IV. Sequential Development of Resistances to Chemical and Physical Agents during Sporulation of *Bacillus subtilis*. *Mol. Gen. Genet.* **1973**, *125* (3), 241–250.
- (59) Mason, J. M.; Setlow, P. Essential Role of Small, Acid-Soluble Spore Proteins in Resistance of *Bacillus subtilis* Spores to UV Light. *J. Bacteriol.* **1986**, *167* (1), 174–178.
- (60) Jenkinson, H. F.; Sawyer, W. D.; Mandelstam, J. Synthesis and Order of Assembly of Spore Coat Proteins in *Bacillus subtilis*. *Microbiology* **1981**, *123* (1), 1–16.
- (61) Cano, R. J.; Borucki, M. K. Revival and Identification of Bacterial Spores in 25- to 40-Million-Year-Old Dominican Amber. *Science* **1995**, *268* (5213), 1060–1064.
- (62) Tetz, V. V.; Rybalchenko, O. V.; Savkova, G. A. Ultrastructural Features of Microbial Colony Organization. *J. Basic Microbiol.* **1990**, *30* (8), 597–607.
- (63) Fiocca, R.; Necchi, V.; Sommi, P.; Ricci, V.; Telford, J.; Cover, T. L.; Solcia, E. Release of *Helicobacter pylori* Vacuolating Cytotoxin by Both a Specific Secretion Pathway and Budding of Outer Membrane Vesicles. Uptake of Released Toxin and Vesicles by Gastric Epithelium. *J. Pathol.* **1999**, *188* (2), 220–226.
- (64) Stephens, D. S.; Edwards, K. M.; Morris, F.; McGee, Z. A. Pili and Outer Membrane Appendages on *Neisseria meningitidis* in the Cerebrospinal Fluid of an Infant. *J. Infect. Dis.* **1982**, *146* (4), 568.
- (65) Loeb, M. R. Bacteriophage T4-Mediated Release of Envelope Components from *Escherichia coli*. *J. Virol.* **1974**, *13* (3), 631–641.

- (66) Knox, K. W.; Vesik, M.; Work, E. Relation between Excreted Lipopolysaccharide Complexes and Surface Structures of a Lysine-Limited Culture of *Escherichia coli*. *J. Bacteriol.* **1966**, 92 (4), 1206–1217.
- (67) Kadurugamuwa, J. L.; Beveridge, T. J. Natural Release of Virulence Factors in Membrane Vesicles by *Pseudomonas aeruginosa* and the Effect of Aminoglycoside Antibiotics on Their Release. *J. Antimicrob. Chemother.* **1997**, 40 (5), 615–621.
- (68) Chutkan, H.; Macdonald, I.; Manning, A.; Kuehn, M. J. Quantitative and Qualitative Preparations of Bacterial Outer Membrane Vesicles. *Methods Mol. Biol.* **2013**, 966, 259–272.
- (69) Taylor, D. D.; Shah, S. Methods of Isolating Extracellular Vesicles Impact down-Stream Analyses of Their Cargoes. *Methods* **2015**.
- (70) Ferrari, G.; Garaguso, I.; Adu-Bobie, J.; Doro, F.; Taddei, A. R.; Biolchi, A.; Brunelli, B.; Giuliani, M. M.; Pizza, M.; Norais, N.; et al. Outer Membrane Vesicles from Group B *Neisseria meningitidis* Delta gna33 Mutant: Proteomic and Immunological Comparison with Detergent-Derived Outer Membrane Vesicles. *Proteomics* **2006**, 6 (6), 1856–1866.
- (71) Horstman, A. L.; Kuehn, M. J. Enterotoxigenic *Escherichia Coli* Secretes Active Heat-Labile Enterotoxin via Outer Membrane Vesicles. *J. Biol. Chem.* **2000**, 275 (17), 12489–12496.
- (72) Witwer, K. W.; Buzás, E. I.; Bemis, L. T.; Bora, A.; Lässer, C.; Lötvall, J.; Nolte-'t Hoen, E. N.; Piper, M. G.; Sivaraman, S.; Skog, J.; et al. Standardization of Sample Collection, Isolation and Analysis Methods in Extracellular Vesicle Research. *J. Extracell. vesicles* **2013**, 2.
- (73) Van de Waterbeemd, B.; Zomer, G.; Kaaijk, P.; Ruitkamp, N.; Wijffels, R. H.; van den Dobbelsteen, G. P. J. M.; van der Pol, L. A. Improved Production Process for Native Outer Membrane Vesicle Vaccine against *Neisseria meningitidis*. *PLoS One* **2013**, 8 (5), e65157.
- (74) Böing, A. N.; van der Pol, E.; Grootemaat, A. E.; Coumans, F. A. W.; Sturk, A.; Nieuwland, R. Single-Step Isolation of Extracellular Vesicles by Size-Exclusion Chromatography. *J. Extracell. vesicles* **2014**, 3.
- (75) Taylor, D. D.; Zacharias, W.; Gercel-Taylor, C. Exosome Isolation for Proteomic Analyses and RNA Profiling. *Methods Mol. Biol.* **2011**, 728, 235–246.

- (76) Tian, T.; Wang, Y.; Wang, H.; Zhu, Z.; Xiao, Z. Visualizing of the Cellular Uptake and Intracellular Trafficking of Exosomes by Live-Cell Microscopy. *J. Cell. Biochem.* **2010**, *111* (2), 488–496.
- (77) Sterlini, J. M.; Mandelstam, J. Commitment to Sporulation in *Bacillus subtilis* and Its Relationship to Development of Actinomycin Resistance. *Biochem. J.* **1969**, *113* (1), 29–37.
- (78) Schaeffer, A. B.; Fulton, M. D. A Simplified Method of Staining Endospores. *Science* **1933**, *77* (1990), 194.
- (79) McBroom, A. J.; Johnson, A. P.; Vemulapalli, S.; Kuehn, M. J. Outer Membrane Vesicle Production by *Escherichia coli* Is Independent of Membrane Instability. *J. Bacteriol.* **2006**, *188* (15), 5385–5392.
- (80) Spurr, A. R. A Low-Viscosity Epoxy Resin Embedding Medium for Electron Microscopy. *J. Ultrastruct. Res.* **1969**, *26* (1), 31–43.
- (81) Chaiyanan, S.; Chaiyanan, S.; Grim, C.; Mangel, T.; Huq, A.; Colwell, R. R. Ultrastructure of Coccoid Viable but Non-Culturable *Vibrio cholerae*. *Environ. Microbiol.* **2007**, *9* (2), 393–402.
- (82) Théry, C.; Amigorena, S.; Raposo, G.; Clayton, A. Isolation and Characterization of Exosomes from Cell Culture Supernatants and Biological Fluids. *Curr. Protoc. Cell Biol.* **2006**, *Chapter 3*, Unit 3.22.
- (83) Schneider, C. A.; Rasband, W. S.; Eliceiri, K. W. NIH Image to ImageJ: 25 Years of Image Analysis. *Nat. Methods* **2012**, *9* (7), 671–675.
- (84) Kong, M.; Bhattacharya, R. N.; James, C.; Basu, A. A Statistical Approach to Estimate the 3D Size Distribution of Spheres from 2D Size Distributions. *Geol. Soc. Am. Bull.* **2005**, *117* (1), 244.
- (85) Hong, S.-W.; Kim, M.-R.; Lee, E.-Y.; Kim, J. H.; Kim, Y.-S.; Jeon, S. G.; Yang, J.-M.; Lee, B.-J.; Pyun, B.-Y.; Gho, Y. S.; et al. Extracellular Vesicles Derived from *Staphylococcus aureus* Induce Atopic Dermatitis-like Skin Inflammation. *Allergy* **2011**, *66* (3), 351–359.
- (86) Kim, J. H.; Lee, J.; Park, J.; Gho, Y. S. Gram-Negative and Gram-Positive Bacterial Extracellular Vesicles. *Semin. Cell Dev. Biol.* **2015**.
- (87) Aebersold, R.; Mann, M. Mass Spectrometry-Based Proteomics. *Nature* **2003**, *422* (6928), 198–207.
- (88) Zhang, Z.; Wu, S.; Stenoien, D. L.; Paša-Tolić, L. High-Throughput Proteomics. *Annu. Rev. Anal. Chem. (Palo Alto, Calif.)* **2014**, *7*, 427–454.

- (89) Dass, C. *Fundamentals of Contemporary Mass Spectrometry*; Desiderio, D. M., Ed.; John Wiley & Sons: Hoboken, NJ, 2007.
- (90) Fenn, J. B.; Mann, M.; Meng, C. K.; Wong, S. F.; Whitehouse, C. M. Electrospray Ionization for Mass Spectrometry of Large Biomolecules. *Science* **1989**, *246* (4926), 64–71.
- (91) Smith, R. D.; Loo, J. A.; Loo, R. R. O.; Busman, M.; Udseth, H. R. Principles and Practice of Electrospray Ionization—Mass Spectrometry for Large Polypeptides and Proteins. *Mass Spectrom. Rev.* **1991**, *10* (5), 359–452.
- (92) Makarov, A.; Denisov, E.; Kholomeev, A.; Balschun, W.; Lange, O.; Strupat, K.; Horning, S. Performance Evaluation of a Hybrid Linear Ion Trap/orbitrap Mass Spectrometer. *Anal. Chem.* **2006**, *78* (7), 2113–2120.
- (93) Schwartz, J. C.; Senko, M. W.; Syka, J. E. P. A Two-Dimensional Quadrupole Ion Trap Mass Spectrometer. *J. Am. Soc. Mass Spectrom.* **2002**, *13* (6), 659–669.
- (94) Stafford, G. C.; Kelley, P. E.; Syka, J. E. P.; Reynolds, W. E.; Todd, J. F. J. Recent Improvements in and Analytical Applications of Advanced Ion Trap Technology. *Int. J. Mass Spectrom. Ion Process.* **1984**, *60* (1), 85–98.
- (95) Hu, Q.; Noll, R. J.; Li, H.; Makarov, A.; Hardman, M.; Graham Cooks, R. The Orbitrap: A New Mass Spectrometer. *J. Mass Spectrom.* **2005**, *40* (4), 430–443.
- (96) Cannon, J. R.; Edwards, N. J.; Fenselau, C. Mass-Biased Partitioning to Enhance Middle down Proteomics Analysis. *J. Mass Spectrom.* **2013**, *48* (3), 340–343.
- (97) Wu, C. C.; MacCoss, M. J. Shotgun Proteomics: Tools for the Analysis of Complex Biological Systems. *Curr. Opin. Mol. Ther.* **2002**, *4* (3), 242–250.
- (98) Alves, P.; Arnold, R. J.; Novotny, M. V.; Radivojac, P.; Reilly, J. P.; Tang, H. Advancement in Protein Inference from Shotgun Proteomics Using Peptide Detectability. *Pac. Symp. Biocomput.* **2007**, 409–420.
- (99) Sleno, L.; Volmer, D. A. Ion Activation Methods for Tandem Mass Spectrometry. *J. Mass Spectrom.* **2004**, *39* (10), 1091–1112.
- (100) Nesvizhskii, A. I.; Aebersold, R. Interpretation of Shotgun Proteomic Data: The Protein Inference Problem. *Mol. Cell. Proteomics* **2005**, *4* (10), 1419–1440.

- (101) The UniProt Consortium. UniProt: A Hub for Protein Information. *Nucleic Acids Res.* **2014**, gku989 .
- (102) Pruitt, K. D.; Tatusova, T.; Brown, G. R.; Maglott, D. R. NCBI Reference Sequences (RefSeq): Current Status, New Features and Genome Annotation Policy. *Nucleic Acids Res.* **2011**, *40* (D1), D130–D135.
- (103) Perkins, D. N.; Pappin, D. J.; Creasy, D. M.; Cottrell, J. S. Probability-Based Protein Identification by Searching Sequence Databases Using Mass Spectrometry Data. *Electrophoresis* **1999**, *20* (18), 3551–3567.
- (104) Eng, J. K.; McCormack, A. L.; Yates, J. R. An Approach to Correlate Tandem Mass Spectral Data of Peptides with Amino Acid Sequences in a Protein Database. *J. Am. Soc. Mass Spectrom.* **1994**, *5* (11), 976–989.
- (105) Craig, R.; Beavis, R. C. A Method for Reducing the Time Required to Match Protein Sequences with Tandem Mass Spectra. *Rapid Commun. Mass Spectrom.* **2003**, *17* (20), 2310–2316.
- (106) Edwards, N. PepArML: A Meta-Search Peptide Identification Platform for Tandem Mass Spectra. *Curr. Protoc. Bioinforma.* **2013**, *44* (13.23), 1–13.
- (107) Deutsch, E. W.; Lam, H.; Aebersold, R. Data Analysis and Bioinformatics Tools for Tandem Mass Spectrometry in Proteomics. *Physiol. Genomics* **2008**, *33* (1), 18–25.
- (108) Lam, H.; Deutsch, E. W.; Eddes, J. S.; Eng, J. K.; King, N.; Stein, S. E.; Aebersold, R. Development and Validation of a Spectral Library Searching Method for Peptide Identification from MS/MS. *Proteomics* **2007**, *7* (5), 655–667.
- (109) Käll, L.; Storey, J. D.; MacCoss, M. J.; Noble, W. S. Assigning Significance to Peptides Identified by Tandem Mass Spectrometry Using Decoy Databases. *J. Proteome Res.* **2008**, *7* (1), 29–34.
- (110) Benjamini, Y.; Hochberg, Y. Controlling the False Discovery Rate: A Practical and Powerful Approach to Multiple Testing. *J. R. Stat. Soc. Ser. B* **1995**, *57*, 289–300.
- (111) Elias, J. E.; Gygi, S. P. Target-Decoy Search Strategy for Increased Confidence in Large-Scale Protein Identifications by Mass Spectrometry. *Nat. Methods* **2007**, *4* (3), 207–214.
- (112) Gupta, N.; Pevzner, P. A. False Discovery Rates of Protein Identifications: A Strike against the Two-Peptide Rule. *J. Proteome Res.* **2009**, *8* (9), 4173–4181.



- (113) Bantscheff, M.; Schirle, M.; Sweetman, G.; Rick, J.; Kuster, B. Quantitative Mass Spectrometry in Proteomics: A Critical Review. *Anal. Bioanal. Chem.* **2007**, *389* (4), 1017–1031.
- (114) Bantscheff, M.; Lemeer, S.; Savitski, M. M.; Kuster, B. Quantitative Mass Spectrometry in Proteomics: Critical Review Update from 2007 to the Present. *Anal. Bioanal. Chem.* **2012**, *404* (4), 939–965.
- (115) Thompson, A.; Schäfer, J.; Kuhn, K.; Kienle, S.; Schwarz, J.; Schmidt, G.; Neumann, T.; Johnstone, R.; Mohammed, A. K. A.; Hamon, C. Tandem Mass Tags: A Novel Quantification Strategy for Comparative Analysis of Complex Protein Mixtures by MS/MS. *Anal. Chem.* **2003**, *75* (8), 1895–1904.
- (116) Ross, P. L.; Huang, Y. N.; Marchese, J. N.; Williamson, B.; Parker, K.; Hattan, S.; Khainovski, N.; Pillai, S.; Dey, S.; Daniels, S.; et al. Multiplexed Protein Quantitation in *Saccharomyces Cerevisiae* Using Amine-Reactive Isobaric Tagging Reagents. *Mol. Cell. Proteomics* **2004**, *3* (12), 1154–1169.
- (117) Wiese, S.; Reidegeld, K. A.; Meyer, H. E.; Warscheid, B. Protein Labeling by iTRAQ: A New Tool for Quantitative Mass Spectrometry in Proteome Research. *Proteomics* **2007**, *7* (3), 340–350.
- (118) Ong, S.-E. Stable Isotope Labeling by Amino Acids in Cell Culture, SILAC, as a Simple and Accurate Approach to Expression Proteomics. *Mol. Cell. Proteomics* **2002**, *1* (5), 376–386.
- (119) Liu, H.; Sadygov, R. G.; Yates, J. R. A Model for Random Sampling and Estimation of Relative Protein Abundance in Shotgun Proteomics. *Anal. Chem.* **2004**, *76* (14), 4193–4201.
- (120) Old, W. M.; Meyer-Arendt, K.; Aveline-Wolf, L.; Pierce, K. G.; Mendoza, A.; Sevinsky, J. R.; Resing, K. A.; Ahn, N. G. Comparison of Label-Free Methods for Quantifying Human Proteins by Shotgun Proteomics. *Mol. Cell. Proteomics* **2005**, *4* (10), 1487–1502.
- (121) Dennis, G. J.; Sherman, B. T.; Hosack, D. A.; Yang, J.; Gao, W.; Lane, H. C.; Lempicki, R. A. DAVID: Database for Annotation, Visualization, and Integrated Discovery. *Genome Biol.* **2003**, *4* (5), P3.
- (122) Lowry, O. H. Micromethods for the Assay of Enzyme. II Specific Procedures. Alkaline Phosphatase. *Methods Enzymol.* **1955**, 371–372.
- (123) Stover, A. G.; Driks, A. Secretion, Localization, and Antibacterial Activity of TasA, a *Bacillus subtilis* Spore-Associated Protein. *J. Bacteriol.* **1999**, *181* (5), 1664–1672.

- (124) Perego, M.; Higgins, C. F.; Pearce, S. R.; Gallagher, M. P.; Hoch, J. A. The Oligopeptide Transport System of *Bacillus subtilis* Plays a Role in the Initiation of Sporulation. *Mol. Microbiol.* **1991**, *5* (1), 173–185.
- (125) Rudner, D. Z.; LeDeaux, J. R.; Ireton, K.; Grossman, A. D. The spo0K Locus of *Bacillus subtilis* Is Homologous to the Oligopeptide Permease Locus and Is Required for Sporulation and Competence. *J. Bacteriol.* **1991**, *173* (4), 1388–1398.
- (126) LeDeaux, J. R.; Solomon, J. M.; Grossman, A. D. Analysis of Non-Polar Deletion Mutations in the Genes of the spo0K (opp) Operon of *Bacillus subtilis*. *FEMS Microbiol. Lett.* **1997**, *153* (1), 63–69.
- (127) Fawcett, P.; Eichenberger, P.; Losick, R.; Youngman, P. The Transcriptional Profile of Early to Middle Sporulation in *Bacillus Subtilis*. *Proc. Natl. Acad. Sci. U. S. A.* **2000**, *97* (14), 8063–8068.
- (128) Edwards, D. H.; Errington, J. The *Bacillus subtilis* DivIVA Protein Targets to the Division Septum and Controls the Site Specificity of Cell Division. *Mol. Microbiol.* **1997**, *24* (5), 905–915.
- (129) Thomaidis, H. B.; Freeman, M.; El Karoui, M.; Errington, J. Division Site Selection Protein DivIVA of *Bacillus subtilis* Has a Second Distinct Function in Chromosome Segregation during Sporulation. *Genes Dev.* **2001**, *15* (13), 1662–1673.
- (130) Cha, J. H.; Stewart, G. C. The divIVA Minicell Locus of *Bacillus subtilis*. *J. Bacteriol.* **1997**, *179* (5), 1671–1683.
- (131) Siranosian, K. J.; Ireton, K.; Grossman, A. D. Alanine Dehydrogenase (ald) Is Required for Normal Sporulation in *Bacillus subtilis*. *J. Bacteriol.* **1993**, *175* (21), 6789–6796.
- (132) Dubnau, E. J.; Cabane, K.; Smith, I. Regulation of spo0H, an Early Sporulation Gene in *bacilli*. *J. Bacteriol.* **1987**, *169* (3), 1182–1191.
- (133) Hulett, F. M.; Bookstein, C.; Jensen, K. Evidence for Two Structural Genes for Alkaline Phosphatase in *Bacillus subtilis*. *J. Bacteriol.* **1990**, *172* (2), 735–740.
- (134) Miller, J. H. Assay of Beta-Galactosidase. In *Experiments in Molecular Genetics*; Cold Spring Harbor Laboratory Press: Cold Spring Harbor, NY, 1972; pp 352–355.
- (135) Bookstein, C.; Edwards, C. W.; Kapp, N. V.; Hulett, F. M. The *Bacillus subtilis* 168 Alkaline Phosphatase III Gene: Impact of a phoAIII Mutation on Total Alkaline Phosphatase Synthesis. *J. Bacteriol.* **1990**, *172* (7), 3730–3737.

- (136) Levin, P. A.; Losick, R. Characterization of a Cell Division Gene from *Bacillus subtilis* That Is Required for Vegetative and Sporulation Septum Formation. *J. Bacteriol.* **1994**, *176* (5), 1451–1459.
- (137) Knurr, J.; Benedek, O.; Heslop, J.; Vinson, R. B.; Boydston, J. A.; McAndrew, J.; Kearney, J. F.; Turnbough, C. L. Peptide Ligands That Bind Selectively to Spores of *Bacillus subtilis* and Closely Related Species. *Appl. Environ. Microbiol.* **2003**, *69* (11), 6841–6847.
- (138) Krogh, S.; O'Reilly, M.; Nolan, N.; Devine, K. M. The Phage-like Element PBSX and Part of the Skin Element, Which Are Resident at Different Locations on the *Bacillus subtilis* Chromosome, Are Highly Homologous. *Microbiology* **1996**, *142*, 2031–2040.
- (139) Lauber, M. A.; Running, W. E.; Reilly, J. P. *B. subtilis* Ribosomal Proteins: Structural Homology and Post-Translational Modifications. *J. Proteome Res.* **2009**, *8* (9), 4193–4206.
- (140) Hanlon, D. W.; Ordal, G. W. Cloning and Characterization of Genes Encoding Methyl-Accepting Chemotaxis Proteins in *Bacillus subtilis*. *J. Biol. Chem.* **1994**, *269* (19), 14038–14046.
- (141) Morelli, A. E.; Larregina, A. T.; Shufesky, W. J.; Sullivan, M. L. G.; Stolz, D. B.; Papworth, G. D.; Zahorchak, A. F.; Logar, A. J.; Wang, Z.; Watkins, S. C.; et al. Endocytosis, Intracellular Sorting, and Processing of Exosomes by Dendritic Cells. *Blood* **2004**, *104* (10), 3257–3266.
- (142) Tian, T.; Zhu, Y.-L.; Hu, F.-H.; Wang, Y.-Y.; Huang, N.-P.; Xiao, Z.-D. Dynamics of Exosome Internalization and Trafficking. *J. Cell. Physiol.* **2013**, *228* (7), 1487–1495.
- (143) Lonhienne, T. G. A.; Sagulenko, E.; Webb, R. I.; Lee, K.-C.; Franke, J.; Devos, D. P.; Nouwens, A.; Carroll, B. J.; Fuerst, J. A. Endocytosis-like Protein Uptake in the Bacterium *Gemmata Obscuriglobus*. *Proc. Natl. Acad. Sci. U. S. A.* **2010**, *107* (29), 12883–12888.
- (144) Bomberger, J. M.; Maceachran, D. P.; Coutermarsh, B. A.; Ye, S.; O'Toole, G. A.; Stanton, B. A. Long-Distance Delivery of Bacterial Virulence Factors by *Pseudomonas Aeruginosa* Outer Membrane Vesicles. *PLoS Pathog.* **2009**, *5* (4), e1000382.
- (145) Sibarita, J.-B. Deconvolution Microscopy. *Adv. Biochem. Eng. Biotechnol.* **2005**, *95*, 201–243.

- (146) Wallace, W.; Schaefer, L. H.; Swedlow, J. R. A Workingperson's Guide to Deconvolution in Light Microscopy. *Biotechniques* **2001**, *31* (5), 1076–1078, 1080, 1082 passim.
- (147) Struck, D. K.; Hoekstra, D.; Pagano, R. E. Use of Resonance Energy Transfer to Monitor Membrane Fusion. *Biochemistry* **1981**, *20* (14), 4093–4099.
- (148) Hoekstra, D.; de Boer, T.; Klappe, K.; Wilschut, J. Fluorescence Method for Measuring the Kinetics of Fusion between Biological Membranes. *Biochemistry* **1984**, *23* (24), 5675–5681.
- (149) Parolini, I.; Federici, C.; Raggi, C.; Lugini, L.; Palleschi, S.; De Milito, A.; Coscia, C.; Iessi, E.; Logozzi, M.; Molinari, A.; et al. Microenvironmental pH Is a Key Factor for Exosome Traffic in Tumor Cells. *J. Biol. Chem.* **2009**, *284* (49), 34211–34222.
- (150) Harry, E. J.; Pogliano, K.; Losick, R. Use of Immunofluorescence to Visualize Cell-Specific Gene Expression during Sporulation in *Bacillus subtilis*. *J. Bacteriol.* **1995**, *177* (12), 3386–3393.
- (151) Montecalvo, A.; Larregina, A. T.; Shufesky, W. J.; Stolz, D. B.; Sullivan, M. L. G.; Karlsson, J. M.; Baty, C. J.; Gibson, G. A.; Erdos, G.; Wang, Z.; et al. Mechanism of Transfer of Functional microRNAs between Mouse Dendritic Cells via Exosomes. *Blood* **2012**, *119* (3), 756–766.
- (152) Encyclopædia britannica. Schematic drawing of the structure of a typical bacterial cell of the bacillus type.  
<http://www.britannica.com/EBchecked/media/707/Schematic-drawing-of-the-structure-of-a-typical-bacterial-cell>.